Analytica Chimica Acta 1237 (2023) 340591

Contents lists available at ScienceDirect

Analytica Chimica Acta

journal homepage: www.elsevier.com/locate/aca

Microfluidic electrochemical device for real-time culturing and interference-free detection of *Escherichia coli*

Sonal Fande [a,c], Khairunnisa Amreen [a,b], D. Sriram [c], Sanket Goel [a,b,*]

[a] MEMS, Microfluidics and Nanoelectronics Lab, Department of Electrical and Electronics Engineering, Birla Institute of Technology and Science, Hyderabad, 500078, India
[b] Department of Electrical and Electronics Engineering, Birla Institute of Technology and Science, Hyderabad, 500078, India
[c] Department of Pharmacy, Birla Institute of Technology and Science, Hyderabad, 500078, India

HIGHLIGHTS

- A novel microfluidic electrochemical device for *E. Coli* detection is presented.
- Incubator-free bacteria culturing and monitoring of the growth were achieved.
- A linear bacterial concentration ranges of 0.336–40 CFU/fL was attained.
- A detection limit of 0.35 CFU mL^{-1} was achieved.
- The platform continuously monitors the bacterial growth even in real sample.

GRAPHICAL ABSTRACT

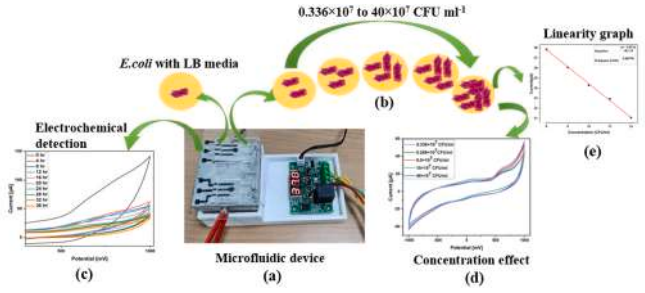

ARTICLE INFO

Keywords:
Escherichia coli
Graphitized-mesoporous carbon
Electrochemical detection
Lab on chip
Microfluidic device
Point of care treatment

ABSTRACT

Bacterial contamination and infection is a major health concern today leading to the significance of its detection. Being lab-based bacterial culturing processes, the present approaches are time consuming and require trained skillset. An economical, and miniaturized lab-on-chip device, capable of simultaneous detection of bacterial growth, could be a benchmarking tool for monitoring the bacterial contamination. Herein, the microfluidic-based electrochemical device for a fast, susceptible, detection of *Escherichia coli* was developed. The device could aid incubator free bacteria culturing in the ambient atmosphere and simultaneously monitor and detect the growth electrochemically. A three-electrode system, integrated with a reservoir and a portable thermostat temperature controller was fabricated and assembled. To achieve this, three-electrodes were embedded on the microfluidic device by screen-printing carbon paste, and the working electrode was enhanced by graphitized mesoporous carbon. Cyclic voltammetry response was noted as the function of concentration and growth of *Escherichia Coli* in the reservoir. The device gave a linear bacterial concentration range of 0.336×10^{12} to 40×10^{12} CFU mL^{-1}, detection limit of 0.35 CFU mL^{-1} and the quantification limit of 1.05 CFU mL^{-1} which was less than the maximum allowable limit. The developed platform was further used to detect and continuously monitor the bacterial growth in the real sample (mango juice) for a period of 36 h. Finally, the

* Corresponding author. MEMS, Microfluidics and Nanoelectronics Lab, Department of Electrical and Electronics Engineering, Birla Institute of Technology and Science, Hyderabad, 500078, India.
E-mail address: sgoel@hyderabad.bits-pilani.ac.in (S. Goel).

https://doi.org/10.1016/j.aca.2022.340591
Received 13 October 2022; Accepted 2 November 2022
Available online 5 November 2022

interference from other common bacteria on the electrode selectivity was also investigated. Such approach in being further modified for specific sensing of bacteria in patients suffering from different diseases such as corneal ulcers, Diarrhea, tuberculosis, leprosy, and syphilis.

1. Introduction

Bacterial infection is a worldwide health concern. It causes significant morbidity and mortality, especially for those who are vulnerable [1]. With septic shocks, every hour of antibiotic treatment delay raises the risk of death of patient by 7.65% [2]. Failure to treat bacterial infections in their early and vital stages can be harmful due to their virulence factor, highlighting the need for new treatments to develop [3]. To evaluate the bacterial concentration, many approaches are utilized, such as plating, optical imaging, or biological alterations, which are costly and require expertise in handling. Moreover, their instruments are often bulky, expensive, and difficult to work with and they lack the ability to miniaturize for the point-of-care (POC) applications. The absence of protocol plus procedure uniformity also leads to differences in outcomes. Therefore, there is a pressing demand for diagnostic devices that are compatible with clinical microbiology lab workflow and competent for identifying bacteria concentration and growth in a rapid, real-time, high-throughput, and contact-free manner. [4,5].

Clinical assessment, medical examination, microbiology, biomedical techniques, and diagnostics have all been changed by the introduction of lab-on-chip microfluidic technology. Microfluidic technologies have recently been utilized a solid platform for collective therapeutic applications, together with clinical microbiology owing to inherent characteristics like transportability, minimum patient sample requirements, miniaturizing manual interference, profitable, and increased sensitivity, specificity, and greater output. Through the growing productivity of clinical practices, clinical assessment of serum and urine biochemical testing for resolving contagious diseases, drug development, microbiology, and pathophysiology studies are becoming totally automated [6–14]. After continuous work, microfluidic chip has been developed which can detect bacteria [15]. and its growth with high sensitivity. For microorganism detection, automated microfluidic based DNA extension/purification chip was designed but was less effective and had poor sensitivity. Another article produced a paper-based sensor for bacterial lipopolysaccharide detection, but because being a paper-based device, it is disposable and has limitations to use it for multiplexed analysis [16, 17]. Compare to this, more effective and sensitive as well as being portable device has been developed in this work.

Various bacterial species, like *Pseudomonas, Staphylococcus Aureus*, *Bacillus Cereus*, *Escherichia coli*, *Shewanella Putrefaciens*, and *Streptococcus Pneumoniae,* are the most common bacterial species that causes infection. Amongst these, *Escherichia coli* is the greatest prevalent microorganism with the maximum rate of infection and difficulties [18]. The bacterium *Escherichia coli* is a cylindrical-shaped pathogen that usually originates in the environment [19]. These pathogens can be found in contaminated food and untreated water, as well as in the open environment. Although the majority of *E. Coli* bacteria are considered symbiotic, a few have negative effects on human and animal health [20]. Diarrhea, fever, vomiting, and stomach cramps are all symptoms of *E. coli* infections [21]. *E. coli* survive without oxygen and is commonly present in the large intestine of humans. Their excess presence in the body can result in catastrophic illnesses such as meningitis, anemia, urinary tract infection, corneal ulcer, and kidney failure [22].

Food and drug administration regulatory authorities and manufacturers have undertaken numerous efforts to reduce the risk of foodborne diseases by adapting good manufacturing practices and safety hazards analysis, and risk assessment programs [23]. Nonetheless, minimizing the occurrence of microbial contamination is a difficult task. As a result, detection methods plays an important role in preventing and identifying foodborne infections.

Polymerase chain reaction (PCR) [24], Surface plasma resonance (SPR), [25] Enzyme-linked immunosorbent assay (ELISA) [26], Surface-enhanced Raman scattering (SERS) [27], Microarrays, and biosensor [28]. are some of the new laboratory techniques that have emerged in recent years. In contrast, while the present methods are precise and more prone, the high cost, schedule commitment, also specialized person requirements makes it difficult to put them to use in the field. To address these complications, new, simple, low cost, and effective technologies for detecting bacteria are required. Recent electrochemical approaches can be used in conjunction with bacterial cultivation. Electrochemical detection is becoming more common due to its benefits, which include faster analysis times, higher sensitivity, and fewer samples required. Hence, several reports are present in the literature for detection of *E. coli*. Table 1 gives the summary of some of the recent advances in this context.

This research presents a streamlined process of bacterial detection and growth monitoring in diverse conditions. The bacteria *E. Coli* of $DH_5\alpha$ strain with an optical density (OD-0.10) concentration of $0.336–40 \times 10^7$ were injected into the microfluidic reservoir and placed over the aluminum block. Aluminum block with heater and temperature sensor revealed significant potential for temperature monitoring. The present controller-based thermostat maintains a constant temperature of 37^oC. The developed microfluidic device was placed over the aluminum block whereby two holes at its ends were used as a heating medium. One of the ends was equipped with a heater, which constantly provides heat while the other has a temperature sensor, which senses the temperature. The system was equipped with a feedback system that cuts off the heater once the required temperature is attained. The alligator clips are connected to the electrode and cyclic voltammetry testing is performed [36,

Table 1
Several published publications describing electrochemical measurement of Escherichia coli utilising various electrodes and the electroanalytical methods were compared.

Method	Electrode Used	Concentration range (CFU mL^{-1})	LOD (CFU mL^{-1})	Analysis time (Minutes)	References
CV, CA	Ni foil	6.4×10^4 to 3.3×10^9	10^4	–	[29]
CV.CA	Au electrode array	1.5×10^5 to 1.7×10^6	10^3–10^4	8 min	[22]
EIS	3D gold Nano/ micro islands	1×10^2 to 1×10^4	2×10–1×10^5	–	[30]
EIS	Platinum electrode	10^2 to 10^5	10^2	10 min	[31]
CV	PI-5-CA/C-SWCNT	2.98×10^1–2.98×10^7	2.5	–	[32]
CV	ITO/PET	1×10^3 to 1×10^9	–	30 min	[33]
SWASV	PPCPE	1×10^3 to 1×10^7	8×10^2		[34]
CV, SWV	GMC	2.52×10^3 to 25.2×10^4	50.40	30 min	[35]
CV	GMC	0.336×10^{12} to 40×10^{12}	0.35	–	This work

CV: Cyclic voltammetry, CA: Chrono amperometry, EIS: Electrochemical impedance spectroscopy, PI-5-CA: Poly-5-carboxy acid, C-SWCNT: Carboxylated single-walled carbon nanotubes, ITO/PET: Indium tin oxide/polyethylene terephthalate, SWASV: Square wave anodic stripping voltammetry, PPCPE: Porous pseudo carbon paste electrode, SWV: Square Wave Voltammetry, GMC: Graphitized mesoporous carbon.

37].

Herein, an electrochemical detection was used to detect the growth and concentration of bacteria. The benefits of this study includes real-time, contactless, precise, and consistent detection of bacteria concentration in a range of microbial analyses. graphitized mesoporous carbon (GMC) was used to modify working electrode. GMC is a porous carbon nanomaterial. possessing characteristic physicochemical features and large surface area. The screen-printed carbon ink electrode is modified with GMC and utilized for the measurement of the growth of *Escherichia coli*. The GMC modified electrode has been validated to be a trustworthy and effective method for detecting *E. coli.* For the current study, several critical metrics like repeatability, reproducibility, sensitivity, and stability were perfectly attained. [35] Interaction of other bacteria such as *Shewanella putrefaciens* and *Streptococcus pneumoniae* were also investigated. A real sample analysis with pure mango juice was carried out. This research enables us to continue developing a quick, convenient, and diagnostic tool for the medical investigation of biofluids in microbial study, which may be used for both quick detections of bacterium and evaluation of the interference of bacteria, and the resistance of different antibiotics and the effectiveness of antibiotic using antibiotic susceptibility testing.

2. Methods and materials

2.1. Materials

Purified *Escherichia coli* was obtained from the Biological Science Department, BITS-Pilani, Hyderabad campus. Sodium phosphate monobasic dehydrate (NaH_2PO_4. $2H_2O$), and Sodium phosphate dibasic dehydrate (Na_2HPO_4. H_2O) for pH modification were obtained from S R Life sciences. The growth media like Luria Bertani (LB) Broth and LB broth with agar (Miller) were purchased from Sigma Aldrich. The polydimethylsiloxane (PDMS) and curing agent were acquired from Dow Corning, USA. PVC (polyvinyl chloride) and PMMA (polymethylmethacrylate) sheet were obtained from sigma Aldrich. Conductive carbon paste was procured from Engineered Materials system, Inc. Ag/AgCl was procured from ALS Co. Ltd., Japan, and Graphitized Mesoporous Carbon (GMC) was procured from Sigma Aldrich. Corning microscope slide 70 × 50 mm was kindly provided by Sigma Aldrich. A CO_2 laser (VLS 3.60) was purchased from Universal Laser Systems, AZ, USA.

2.2. Methodology

2.2.1. Fabrication of screen-printed electrodes

Screen printed technique has been used for the fabrication of a three-electrode system. Initially, a mask of the dimension 1000 μm in width with a spacing of 3000 μm between the two electrodes and thickness of 50 μm was prepared. The surface area of the electrode for the electrochemical reaction was around 0.2 mm^2. The mask was prepared on polyvinyl chloride (PVC) sheet adhered to a glass substrate using a CO_2 laser system. After that, using a squeegee, the carbon paste was applied over a mask. Subsequently, the substrate was kept in a hot air oven at 65° c for 60 min. After dying, the PVC sheet was removed leaving the three-electrode substrate on the glass slide. The conductivity of electrode was identified as 3.06×10^3 S/m. Scheme 1 displays the schematic of the fabrication method of screen-printed electrodes. In order to perform electrochemical analysis, from three electrodes one was modified with Ag/AgCl ink, to work as a reference electrode. Another electrode was modified with GMC as a working electrode and screen-printed carbon ink was a counter electrode. The electrodes were placed in the hot air oven at 65 °C for a period of 15 min for drying.

2.2.2. Microfluidic device fabrication

A microfluidic device was made of PDMS and glass substrate due to their durability and well-studied performance as a microfluidic device. The reservoir was 2 mm wide,17 mm in height, and 1.4 mm in length with a capacity of handling 476 μl of fluid. First, the design of the reservoir was prepared in CorelDraw software. The pattern was cut on a PMMA using a CO_2 laser. The microfluidic reservoir was prepared from a 10:1 ratio of PDMS to the curing agent. The unwanted gas was removed from mixture using desiccator. The PDMS polymer was transferred into the mould and heated at 65°C for 1 h. The reservoir was engraved out and 2 mm punches were drilled into the hardened polymer using a blunt needle and was bonded to the glass slide with screen-printed electrodes by treating the surfaces in the presence of oxygen plasma. The real image of the final microfluidic device with the integrated electrodes is shown in Fig. 1.

2.2.3. Fabrication of heater based on aluminium block

An aluminum block with two holes at its ends is used as a heating medium. One of the ends is equipped with a heater, while the other has a temperature sensor. The system is equipped with a feedback system that

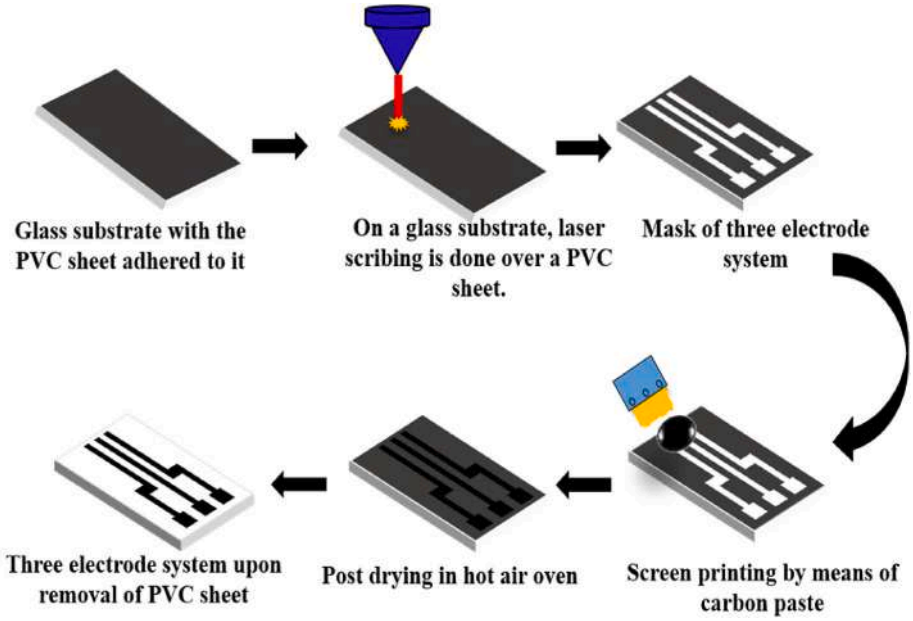

Scheme 1. A step-wise process for fabrication of a screen-printed three-electrode system.

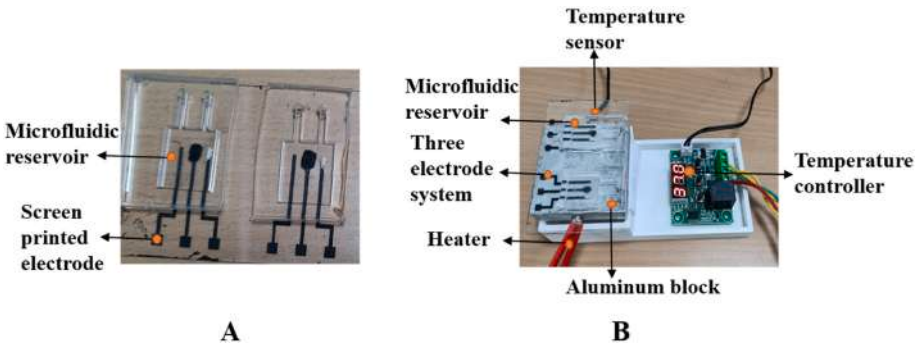

Fig. 1. (A) Microfluidic reservoir bonded to the modified screen-printed electrode (Three-electrode system, working electrode modified with GMC and reference electrode with Ag/AgCl) over the glass slide using plasma treatment (B) the microfluidic device integrated with screen-printed electrodes, aluminum block and thermal management system (Heater and temperature sensor) supported by the controller.

cuts off the heater once the required temperature is attained [36].

2.2.4. Experimental setup of the device

The microfluidic-based reservoir was secured onto the aluminum block with the help of an adhesive tape. The heater and temperature sensor were connected to the Aluminum block. The minimum voltage (12v) was provided through a direct current (DC) voltage booster. The temperature was maintained at 37°C for all sets of experiments. The entire setup can be seen in Fig. 1. The heat generated at this temperature was efficient to grow bacteria.

2.2.5. Bacterial sample preparation

The bacterium species utilized in this experiment was the *E. coli* $DH_5\alpha$ strain. During the preparation, 200 μl of *E. coli* $DH_5\alpha$ culture was inoculated into a 20 mL LB broth and incubated (37° C, using a continuous shaker at 180 Rotation Per minute) for about 36 h. Eventually, the optical density was determined by a smart digital photo colorimeter. Thereafter, the recently cultured microbial sample was diffused and submerged in a pH 7 phosphate buffer solution (PBS). Finally, the microbial cultured sample was diluted in a different concentration from 0.336×10^7 CFU mL^{-1} to 40×10^7 CFU mL^{-1}. CFU mL^{-1} is the most used unit for measuring *E. coli* bacterial concentration. A colony-forming unit is referred to as a CFU. The current changes on the surface of electrode was recorded as function of concentration.

Scheme 2 displays the diagrammatic representation of the serial dilution and plate count. The primary objective of the serial dilution method is to determine the unknown concentration the of a sample (number of bacterial colonies, organism, bacteria, etc.). A series of dilutions (10^8-10^{12}) were made from the original inoculum and to count the presence of microbes in the solution by a plating method. Six agar plates were prepared 100 μl of the sample was speeded over the agar plate from each diluted tube. The plates were kept in an incubator at 37°C for 12 h and formed colonies were counted by the naked eye (manually). The ideal number of colonies to count in a sample is between 30 and 300. If a plate has more than 300 CFU, colonies would become crowded and overlapping [38]. The CFU can be calculated by,

Number of microorganism(CFU mL^{-1}) = (no. of bacterial colonies × total dilution factor)/ volume of cultured plate in mL

2.3. Electrochemical analysis

A potentiostat (Origaflex 500 from Origalys, France) was employed for the electroanalytical measurement. A screen-printed three-electrode system, comprising of GMC electrode, Ag/AgCl as reference electrode, and carbon ink as a counter electrode, were used throughout the electrochemical analysis. GMC has a large surface area, higher void space, and good heat resistivity, which increases its activity manifold in performing functions [39]. The Phosphate buffered saline (PBS), containing a composition of 2.171 g of sodium phosphate dibasic dehydrate and 1.171 g of sodium phosphate monobasic dihydrate of concentration 0.1 M, was used for measurement. Electrolyte pH 7.4 was modified using 0.2 M sodium hydroxide.

2.4. Detection in the real sample

Food such as juices is often connected with foodborne outbreaks

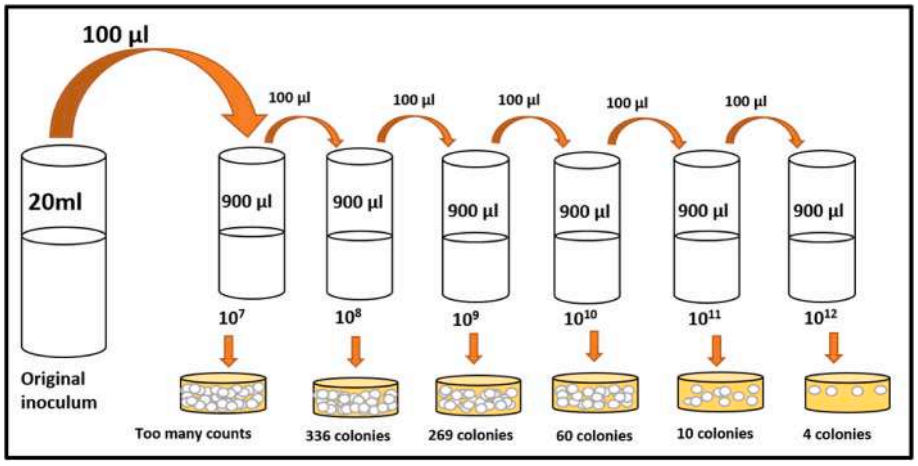

Scheme 2. Diagrammatic picture of serial dilution and plate count.

[40]. Mango juice was procured from the supermarket. The pH of mango juice was adjusted to 6.94. *E. coli* colonies were scraped out from the plate and inoculated in mango juice. The prepared sample was injected into the microfluidic device. Then the electrochemical detection was carried out for the prepared samples.

2.4.1. Field emission scanning electron microscopy characterization of graphitized mesoporous carbon modified electrode

The GMC solution was prepared by the addition of 2 μg of GMC powder to 0.5 mL of 99% ethanol and sonicated for 20 min. Then 0.01 mL of the dispersed solvent was dropped over the screen-printed carbon ink electrode surface and dried in air for 60 min. As a result, sample was ready for the SEM analysis.

3. Results and discussion

3.1. Microscopic study of graphitized mesoporous carbon modified electrode

Fig. 2 illustrates the FESEM (field emission scanning electron microscopy) images of GMC modified electrode. The FESEM examination was carried out to evaluate the physicochemical characterization of diverse nanomaterials, as well as to compute the value of components quantitatively [41]. the image displays that the electrode surface was homogenous and covered with mesoporous carbon.

3.2. Electrochemical analysis of bacteria with graphitized mesoporous carbon

A syringe was used to transport the sample within the microfluidic reservoir. Before the trial, the reservoir was cleaned in 0.1 M PBS (pH 7.4) for 15 min. The prepared bacterial inoculated sample was injected into the microfluidic device and temperature (37 °C) was provided using the thermostat. An electrochemical measurement was directed by means of CV for a period of 36 h at an interval of 4 h to investigate the effect of growth in bacteria with respect to time. Fig. 3(A) shows a voltammogram performed for *E. coli* samples at different time intervals. With time and a constant supply of temperature, the concentration of the bacteria would be multiplying in the microfluidic device. In the graph, the peak

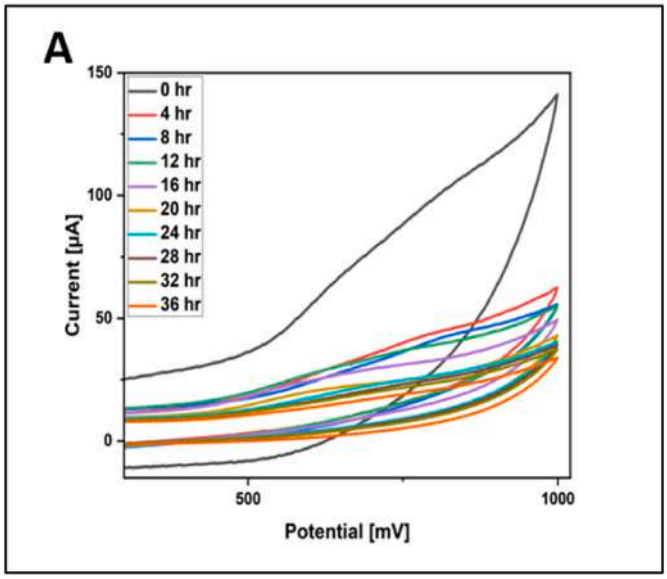

Fig. 3. (A) Cyclic voltammogram recorded for 36 h in microfluidic devices.

current values are gradually reduced with time [33]. Here, the peak current gradually decreases with an increase in time, which must be possible due to an increase in the bacterial concentration in LB media. The reduction of peak current in cyclic voltammetry correspondence to an increase in the incubation time of bacteria [35].

3.3. Concentration effect of Escherichia Coli

For detecting the bacteria in different concentrations, *E. coli* were prepared in PBS buffer (pH 7.44 as well as the Optical density score of 1.12) and inserted onto the microfluidic device. The concentrations of bacteria varied from 0.336×10^{12} to 40×10^{12} CFU mL^{-1} and the cyclic voltammetry was utilized to measure the peak current in the potential range +1 to −1 V, and scan rate of 50 mV s^{-1}. The selected range was sensitive to the GMC electrode below that range detection of bacteria was negligible and above that range, the electrode saturation was

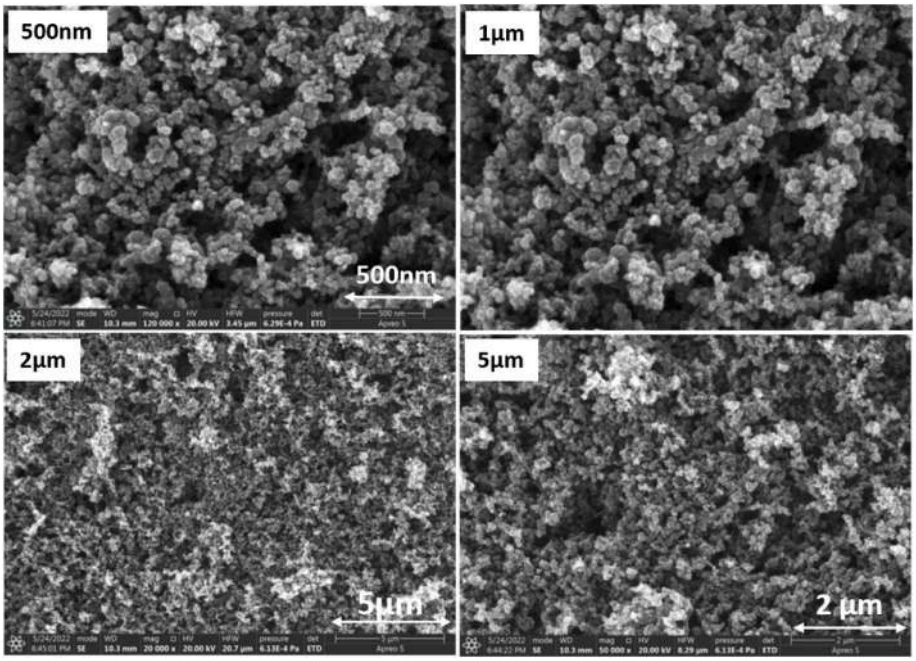

Fig. 2. Microscopic study of GMC modified electrode with different magnification.

observed. Fig. 3(B) shows the CV responses. Herein, the peak current increases as the *E. coli* bacterial concentration raises by *ex-situ* addition. In Fig. 4(A), the lowest concentration was the blue line has the lowest current value. Fig. 4(B) displays the corresponding linear plot relating to the peak current values (μA) and the concentration (CFU mL^{-1}). The correlation coefficient value was determined based on the calibration curve of E_{pa} vs. Conc. The value was observed as $R^2 = 0.997$. This signifies the number of the active site present on the electrode [42]. The limit of detection (LoD)and the limit of quantification (LoQ) were determined using, LoD = 3.3 × σ/slope, LoQ = 10 × σ/slope, and standard deviation represented by σ reported from the least concentration triplicated experiment. The calculated LoD and LoQ of the device are 0.35 and 1.05 CFU mL^{-1} respectively.

3.4. Reproducibility study

To check the consistency of the device the reproducibility study was carried out with different devices. The reproducibility of the device was examined from 6.0×10^7 CFU mL^{-1} of *E. coli*. Electrochemical detection of two devices yielded a reproducible peak current value and the relative standard deviation was 0.41871% (≤10%) presented in Fig. 5(A). The obtained relative standard deviation values redirect the reproducibility of the device.

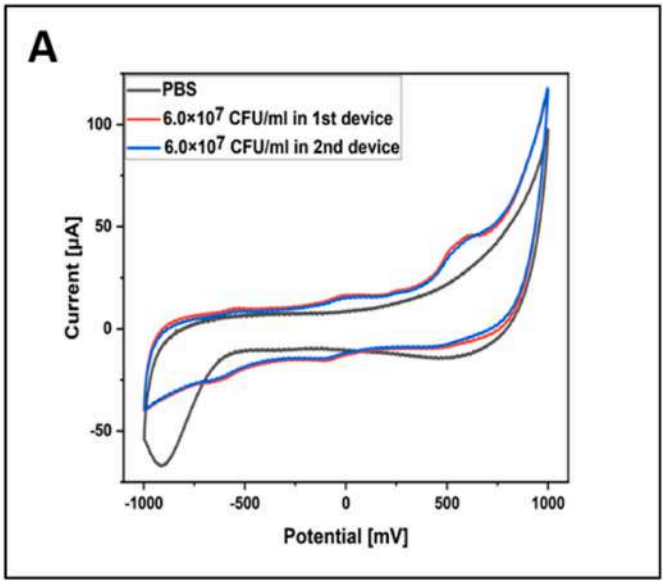

Fig. 5. (A) Cyclic voltammogram for reproducibility study for two different devices.

3.5. Interference study

Interference mitigation in a sensor platform is a vibrant topic for researchers to explore [43]. The specificity of the produced device in detecting *E. coli* was examined. Different variants of bacteria were tested with *E. coli* and in combination with 10^1 CFU mL^{-1} concentration of the selected variant. The same concentration of *Streptococcus Pneumonia* and *Shewanella putrefaciens* was injected into the device and respective peak current responses were evaluated. *Streptococcus Pneumonia* and *Shewanella putrefaciens* are other bacterial species which are quite often associated with infections and food poisoning. Hence, to identify the selectivity of the device in the real time scenario where these similar bacteria may be present, these specific species were chosen Fig. 6 (A and B) demonstrates the corresponding histogram against the *E. coli* and individual variants mixed with *E. coli*. As it can be observed that the bacteria *Streptococcus Pneumonia* and *Shewanella Putrefaciens* don't affect the specificity of the *E. coli* detection.

3.6. Real sample analysis

E. coli is a contagious food microorganism that can effect various organs in human body. A specific difficulty for food manufacturing industry's is that this bacterium may survive in acidic foodstuffs for example, fruit juices, and mayonnaise [44]. The CV measurement was done using real sample including mango juice. Fig. 7 (A&B) shows the signal obtained for the mango juice at different time intervals. As the incubation time increases, the oxidation peak current gradually decreases [32]. Because as incubation period increases, volume of juice reduces, the flow of ions diminishes, and the current value drops. This validates the viability of electrochemical detection in food beverages.

4. Conclusion

Intended for the sensitive measurement as well as culturing of *E. Coli*, herein a simple, easy to fabricate, and a cost-effective miniaturized electrochemical platform with thermal controller has been developed. The developed miniaturized platform was capable of culturing bacteria and detection at the same time. A three electrode system comprised of GMC-modified screen-printed working electrode, Ag/AgCl ink modified screen-printed reference electrode and screen printed carbon ink was the counter electrode. The width of electrode was 1000 μm with a spacing of 3000 μm between the two electrodes and thickness of 50 μm. The use of GMC-modified electrodes improved the sensor sensitivity and surface area. The cyclic voltammetry study was performed to detect bacterial growth. As the raising the concentration, the electrochemical response of *E. coli* bacteria raises. Over the sensing platform LoD, LoQ, reproducibility, and sensitivity were determined. The result demonstrates a linear detection range of *E. coli* concentration of 0.336×10^{12} to 40×10^{12} CFU mL^{-1} with LoD of 0.35 CFU mL^{-1} and LoQ of 1.05 CFU mL^{-1}.

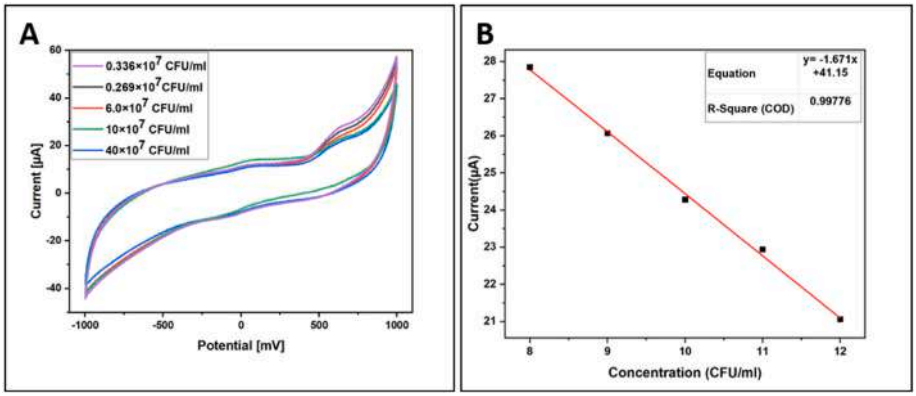

Fig. 4. (A) Cyclic voltammogram of GMC in numerous concentrations of *E. coli* in PBS. (B) Corresponding linear calibration plot for different concentrations.

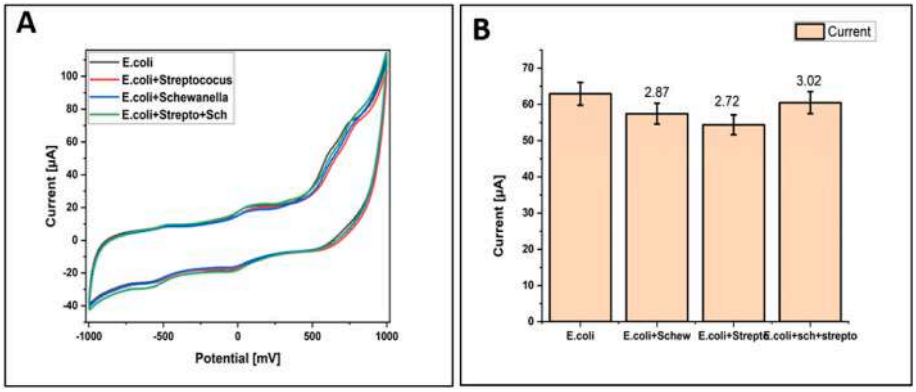

Fig. 6. (A) Cyclic voltammogram for interference study on the modified GMC electrode with two different bacteria (Streptococcus pneumoniae, Shewanella putrefaciens) (B) the Corresponding histogram showing the difference in peak current values associated with *E. coli* and the existence of another interferent of *Shewanella putrefaciens* and *Streptococcus Pneumoniae*.

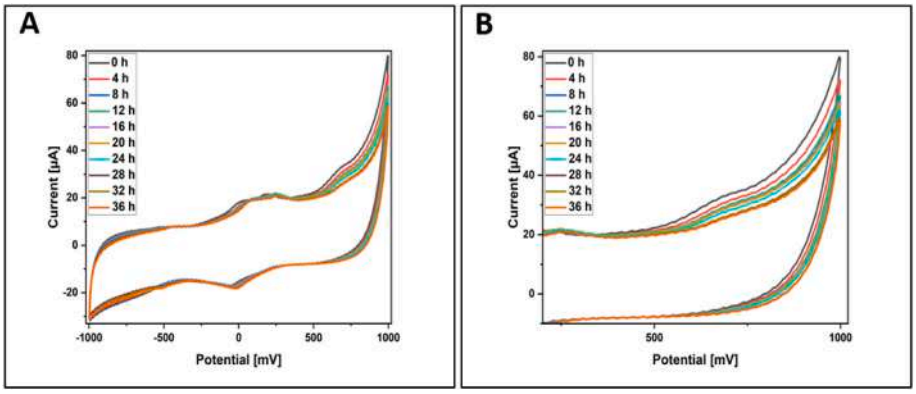

Fig. 7. (A) & (B) Cyclic voltammogram for real sample (fresh mango juice) analysis recorded for 36 h in a microfluidic device in the interval of 4 h. After every 4 h the CV response recorded.

The detected limit has been showed good sensitivity and specificity toward the GMC electrode. GMC significantly increases the overall performance of the sensor and increased the limit of detection 5-fold more than others. The interference study proved the developed sensing platform's high sensitivity toward *E. coli*. The real sample analysis using mango juice was performed showing good reliability.

Declaration of competing interest

The authors declare that they have no known competing financial interests or personal relationships that could have appeared to influence the work reported in this paper.

Data availability

No data was used for the research described in the article.

Acknowledgment

The author thanks Indian council of medical research for funding support (ICMR-SRF scheme 5/3/8/45/ITR-F/2022), and the BITS-Pilani Hyderabad campus central analytical laboratory for characterizations. Dr. Khairunnisa Amreen appreciates the financial support provided by the Department of Health Research (DHR), Indian Council of Medical Research (ICMR), Young Scientist Scheme, YSS/2020/000086. The author thanks Ms. P Ramya Priya and Ms. Himanshi Awasthi for providing a thermostat that is used during experimentation.

References

[1] P. Tandon, G. Garcia-Tsao, Bacterial infections, sepsis, and multiorgan failure in cirrhosis, Semin. Liver Dis. 28 (2008) 26–42, https://doi.org/10.1055/s-2008-1040319.

[2] M.A. Faridi, H. Ramachandraiah, I. Banerjee, S. Ardabili, S. Zelenin, A. Russom, Elasto-inertial microfluidics for bacteria separation from whole blood for sepsis diagnostics, J. Nanobiotechnol. 15 (2017) 1–9, https://doi.org/10.1186/s12951-016-02354.

[3] C. Josenhans, S. Suerbaum, The role of motility as a virulence factor in bacteria, Int. J. Med. Microbiol. 291 (2002) 605–614, https://doi.org/10.1078/1438-4221-00173.

[4] R. Narang, S. Mohammadi, M.M. Ashani, H. Sadabadi, H. Hejazi, M.H. Zarifi, A. Sanati-Nezhad, Sensitive, real-time and non-intrusive detection of concentration and growth of pathogenic bacteria using microfluidic-microwave ring resonator biosensor, Sci. Rep. 8 (2018) 1–10, https://doi.org/10.1038/s41598-018-34001-w.

[5] S. Mahari, S. Gandhi, Recent advances in electrochemical biosensors for the detection of salmonellosis: current prospective and challenges, Biosensors 12 (2022), https://doi.org/10.3390/bios12060365.

[6] H. Madadi, J. Casals-Terré, M. Mohammadi, Self-driven filter-based blood plasma separator microfluidic chip for point-of-care testing, Biofabrication 7 (2015), 25007, https://doi.org/10.1088/1758-5090/7/2/025007.

[7] H. Yang, H. Zhou, H. Hao, Q. Gong, K. Nie, Detection of Escherichia coli with a label-free impedimetric biosensor based on lectin functionalized mixed self-assembled monolayer, Sensor. Actuator. B Chem. 229 (2016) 297–304, https://doi.org/10.1016/j.snb.2015.08.034.

[8] W. Lee, D. Kwon, W. Choi, G.Y. Jung, A.K. Au, A. Folch, S. Jeon, 3D-Printed micro fluidic device for the detection of pathogenic bacteria using size-based separation in helical channel with trapezoid cross-section, Sci. Rep. 5 (2015) 1–7, https://doi.org/10.1038/srep07717.

[9] E. Bojescu, D. Prim, M.E. Pfeifer, J. Segura, Analytica Chimica Acta Fluorescence-polarization immunoassays within glass fiber micro-chambers enable tobramycin quantification in whole blood for therapeutic drug monitoring at the point of care, Anal. Chim. Acta 1225 (2022), 340240, https://doi.org/10.1016/j.aca.2022.340240.

[10] M. Mohammadi, H. Madadi, J. Casals-Terré, Microfluidic point-of-care blood panel based on a novel technique: reversible electroosmotic flow, Biomicrofluidics 9 (2015), https://doi.org/10.1063/1.4930865.
[11] M.H. Zarifi, H. Sadabadi, S.H. Hejazi, M. Daneshmand, A. Sanati-Nezhad, Noncontact and nonintrusive microwave-microfluidic flow sensor for energy and biomedical engineering, Sci. Rep. 8 (2018) 1–10, https://doi.org/10.1038/s41598-017-18621-2.
[12] M. Bahadoran, A.F.A. Noorden, K. Chaudhary, F.S. Mohajer, M.S. Aziz, S. Hashim, J. Ali, P. Yupapin, Modeling and analysis of a microresonating biosensor for detection of salmonella bacteria in human blood, Sensors 14 (2014) 12885–12899, https://doi.org/10.3390/s140712885.
[13] A.M. Kaushik, K. Hsieh, L. Chen, D.J. Shin, J.C. Liao, T.H. Wang, Accelerating bacterial growth detection and antimicrobial susceptibility assessment in integrated picoliter droplet platform, Biosens. Bioelectron. 97 (2017) 260–266, https://doi.org/10.1016/j.bios.2017.06.006.
[14] W. Bin Lee, C.Y. Fu, W.H. Chang, H.L. You, C.H. Wang, M.S. Lee, G. Bin Lee, A microfluidic device for antimicrobial susceptibility testing based on a broth dilution method, Biosens. Bioelectron. 87 (2017) 669–678, https://doi.org/10.1016/j.bios.2016.09.008.
[15] H. Etayash, M.F. Khan, K. Kaur, T. Thundat, Microfluidic cantilever detects bacteria and measures their susceptibility to antibiotics in small confined volumes, Nat. Commun. 7 (2016) 1–9, https://doi.org/10.1038/ncomms12947.
[16] N.C. Cady, S. Stelick, M.V. Kunnavakkam, C.A. Batt, Real-time PCR detection of Listeria monocytogenes using an integrated microfluidics platform, Sensor. Actuator. B Chem. 107 (2005) 332–341, https://doi.org/10.1016/j.snb.2004.10.022.
[17] H. Jiang, J. Yang, K. Wan, D. Jiang, C. Jin, Miniaturized paper-supported 3D cell-based electrochemical sensor for bacterial lipopolysaccharide detection, ACS Sens. 5 (2020) 1325–1335, https://doi.org/10.1021/acssensors.9b02508.
[18] P. Kolhe, A. Roberts, S. Gandhi, Fabrication of an ultrasensitive electrochemical immunosensor coupled with biofunctionalized zero-dimensional graphene quantum dots for rapid detection of cephalexin, Food Chem. 398 (2022), 133846, https://doi.org/10.1016/j.foodchem.2022.
[19] A. Verma, M. Verma, A. Singh, Animal Tissue Culture Principles and Applications, Animal Biotechnology: Models in Discovery and Translation, INC, 2020, https://doi.org/10.1016/B978-0-12-811710-1.00012-4.
[20] L. Viviana Tarditto, M. Alicia Zon, H. García Ovando, N. Roberto Vettorazzi, F. Javier Arévalo, H. Fernández, Electrochemical magneto immunosensor based on endogenous β-galactosidase enzyme to determine enterotoxicogenic Escherichia coli F4 (K88) in swine feces using square wave voltammetry, Talanta 174 (2017) 507–513, https://doi.org/10.1016/j.talanta.2017.06.059.
[21] A. Pandey, Y. Gurbuz, V. Ozguz, J.H. Niazi, A. Qureshi, Graphene-interfaced electrical biosensor for label-free and sensitive detection of foodborne pathogenic E. coli O157:H7, Biosens. Bioelectron. 91 (2017) 225–231, https://doi.org/10.1016/j.bios.2016.12.041.
[22] Z. Altintas, M. Akgun, G. Kokturk, Y. Uludag, A fully automated microfluidic-based electrochemical sensor for real-time bacteria detection, Biosens. Bioelectron. 100 (2018) 541–548, https://doi.org/10.1016/j.bios.2017.09.046.
[23] V. Velusamy, K. Arshak, O. Korostynska, K. Oliwa, C. Adley, An overview of foodborne pathogen detection: in the perspective of biosensors, Biotechnol. Adv. 28 (2010) 232–254, https://doi.org/10.1016/j.biotechadv.2009.12.004.
[24] F.J. Pineda, J.S. Lin, C. Fenselau, P.A. Demirev, Testing the significance of microorganism identification by mass spectrometry and proteome database search, Anal. Chem. 72 (2000) 3739–3744, https://doi.org/10.1021/ac000130q.
[25] R. Maalouf, C. Fournier-Wirth, J. Coste, H. Chebib, Y. Saïkali, O. Vittori, A. Errachid, J.P. Cloarec, C. Martelet, N. Jaffrezic-Renault, Label-free detection of bacteria by electrochemical impedance spectroscopy: comparison to surface plasmon resonance, Anal. Chem. 79 (2007) 4879–4886, https://doi.org/10.1021/ac070085n.
[26] M. Tamminen, T. Joutsjoki, M. Sjöblom, M. Joutsen, A. Palva, E.L. Ryhänen, V. Joutsjoki, Screening of lactic acid bacteria from fermented vegetables by carbohydrate profiling and PCR-ELISA, Lett. Appl. Microbiol. 39 (2004) 439–444, https://doi.org/10.1111/j.1472-765X.2004.01607.x.
[27] W. Gao, B. Li, R. Yao, Z. Li, X. Wang, X. Dong, H. Qu, Q. Li, N. Li, H. Chi, B. Zhou, Z. Xia, Intuitive label-free SERS detection of bacteria using aptamer-based in situ silver nanoparticles synthesis, Anal. Chem. 89 (2017) 9836–9842, https://doi.org/10.1021/acs.analchem.7b01813.
[28] M. Wang, Z. Zheng, Y. Zhang, G. Wang, J. Liu, H. Yu, Analytica Chimica Acta an ultrasensitive label-free electrochemical impedimetric immunosensor for vascular endothelial growth factor based on specific phage via negative, Anal. Chim. Acta 1225 (2022), 340250, https://doi.org/10.1016/j.aca.2022.340250.
[29] A. Ramanujam, B. Neyhouse, R.A. Keogh, M. Muthuvel, R.K. Carroll, G.G. Botte, Rapid electrochemical detection of Escherichia coli using nickel oxidation reaction on a rotating disk electrode, Chem. Eng. J. 411 (2021), 128453, https://doi.org/10.1016/j.cej.2021.128453.
[30] Z. Altintas, M. Akgun, G. Kokturk, Y. Uludag, A fully automated microfluidic-based electrochemical sensor for real-time bacteria detection, Biosens. Bioelectron. 100 (2018) 541–548, https://doi.org/10.1016/j.bios.2017.09.046.
[31] R. Siavash Moakhar, T. Abdelfatah, A. Sanati, M. Jalali, S.E. Flynn, S.S. Mahshid, S. Mahshid, A nanostructured gold/graphene microfluidic device for direct and plasmonic-assisted impedimetric detection of bacteria, ACS Appl. Mater. Interfaces 12 (2020) 23298–23310, https://doi.org/10.1021/acsami.0c02654.
[32] F. Tian, J. Lyu, J. Shi, F. Tan, M. Yang, A polymeric microfluidic device integrated with nanoporous alumina membranes for simultaneous detection of multiple foodborne pathogens, Sensor. Actuator. B Chem. 225 (2016) 312–318, https://doi.org/10.1016/j.snb.2015.11.059.
[33] H. Wang, Y. Fan, Q. Yang, X. Sun, H. Liu, W. Chen, A. Aziz, S. Wang, Boosting the electrochemical performance of PI-5-CA/C-SWCNT nanohybrid for sensitive detection of E. coli O157:H7 from the real sample, Front. Chem. 10 (2022) 1–9, https://doi.org/10.3389/fchem.2022.843859.
[34] J. Sun, A.R. Warden, J. Huang, W. Wang, X. Ding, Colorimetric and electrochemical detection of Escherichia coli and antibiotic resistance based on a p-benzoquinone-mediated bioassay, Anal. Chem. 91 (2019) 7524–7530, https://doi.org/10.1021/acs.analchem.8b04997.
[35] L. Xu, J. Du, Y. Deng, N. He, Electrochemical detection of E. coli O157:H7 using porous pseudo-carbon paste electrode modified with carboxylic multi-walled carbon nanotubes, glutaraldehyde and 3-aminopropyltriethoxysilane, J. Biomed. Nanotechnol. 8 (2012) 1006–1011, https://doi.org/10.1166/jbn.2012.1456.
[36] M.B. Kulkarni, K. Velmurugan, E. Prasanth, K. Amreen, J. Nirmal, S. Goel, Smartphone enabled miniaturized temperature controller platform to synthesize nio/cuo nanoparticles for electrochemical sensing and nanomicelles for ocular drug delivery applications, Biomed. Microdevices 23 (2021) 1–13, https://doi.org/10.1007/s10544-021-00567-y.
[37] M.B. Kulkarni, P.K. Enaganti, K. Amreen, S. Goel, Integrated temperature controlling platform to synthesize ZnO nanoparticles and its deposition on Al-foil for biosensing, IEEE Sensor. J. 21 (2021) 9538–9545, https://doi.org/10.1109/JSEN.2021.3053642.
[38] M. Rishi, K. Amreen, J.M. Mohan, A. Javed, S.K. Dubey, S. Goel, Rapid, sensitive and specific electrochemical detection of E. coli using graphitized mesoporous carbon modified electrodes, Sensors Actuators A Phys 338 (2022), 113483, https://doi.org/10.1016/j.sna.2022.113483.
[39] E.R. Sanders, Aseptic laboratory techniques: plating methods, JoVE 1–18 (2012), https://doi.org/10.3791/3064.
[40] M.M. Rahman, M.G. Ara, M.A. Alim, M.S. Uddin, A. Najda, G.M. Albadrani, A. A. Sayed, S.A. Mousa, M.M. Abdel-Daim, Mesoporous carbon: a versatile material for scientific applications, Int. J. Mol. Sci. 22 (2021), https://doi.org/10.3390/ijms22094498.
[41] D. Wang, J. Chen, S.R. Nugen, Electrochemical detection of Escherichia coli from aqueous samples using engineered phages, Anal. Chem. 89 (2017) 1650–1657, https://doi.org/10.1021/acs.analchem.6b03752.
[42] R. Atchudan, S. Perumal, D. Karthikeyan, A. Pandurangan, Y.R. Lee, Synthesis and characterization of graphitic mesoporous carbon using metal-metal oxide by chemical vapor deposition method, Microporous Mesoporous Mater. 215 (2015) 123–132, https://doi.org/10.1016/j.micromeso.2015.05.032.
[43] J. Sun, A.R. Warden, J. Huang, W. Wang, X. Ding, Colorimetric and electrochemical detection of Escherichia coli and antibiotic resistance based on a p-benzoquinone-mediated bioassay, Anal. Chem. 91 (2019) 7524–7530, https://doi.org/10.1021/acs.analchem.8b04997.
[44] S. Dudala, S.K. Dubey, S. Goel, Microfluidic soil nutrient detection system, IEEE Sens. Counc. 20 (2020) 4504–4511.

Electrochemical Micro-scaled Biosensor for Non-invasive Detection of Lactate

Sonal Fande[1,3], Khairunnisa Amreen1[1,2], Dharmarajan Sriram[3] and Sanket Goel1[1,2]

[1]MEMS, Microfluidic and Nanoelectronic Lab, Department of Electrical and Electronics Engineering, Birla Institute of Technology and Science, Hyderabad 500078, India

[2]Department of Electrical and Electronics Engineering, Birla Institute of Technology and Science, Hyderabad 500078, India

[3]Department of Pharmacy, Birla Institute of Technology and Science, Hyderabad 500078, India

*Corresponding Author: sgoel@hyderabad.bits-pilani.ac.in

2023 16th International Conference on Sensing Technology (ICST) | 979-8-3503-9534-1/23/$31.00 ©2023 IEEE | DOI: 10.1109/ICST59744.2023.10460845

Abstract— **Lactate is a significant biomarker in the anaerobic metabolic pathways of the physiological system. The increase in the level of lactate may lead to disease conditions. It is an essential physical regulator. Lactate is detectable in a range of bodily fluids, such as blood, sweat, plasma, and urine. Among these choices, sweat demonstrates a notable level of concentration. Hence, the feasibility of non-invasive lactate detection has garnered increasing interest and offers a reassuring experience for patients. The present study focuses on the development of an electro-microfluidic device for the non-invasive detection of lactate. The detection platform utilizes an electrochemical sensing system as its foundation. An inkjet-printed electrode improved with multi-walled carbon nanotubes (MWCNT) and functionalized with the Lactate oxidase (LO_x) enzyme. The flexible microfluidic device integrated with a three-electrode system was used for electrochemical sensing lactate levels. The assessment of the enzyme immobilization response was conducted using cyclic voltammetry (CV). The sensor shows a linear range of 1-20 mM concentration with a limit of detection (LoD) and a Limit of Quantification (LoQ) as 1 mM and 3 mM. Due to the inherent flexibility of the electrode, it possesses the capability to be utilized for the purpose of point-of-care lactate detection.**

Keywords- Microfluidic, biosensor, electrochemical, non-invasive

I. INTRODUCTION

The monitoring of lactate levels is imperative in the field of medical diagnosis. The production of a low molecular weight metabolite occurs as a consequence of glycolysis, specifically when the enzyme lactate dehydrogenase catalyzes the conversion of lactate to pyruvate [1]. Lactate metabolites play a crucial role in various physiological processes associated with multiple disease conditions, such as fatigue, sepsis, and hypoxia. It is found within the circulatory system and various biological systems, albeit in a more pronounced concentration within perspiration [2]. The currently accessible lactate sensors in the commercial market are characterized by their invasive nature and the inconvenience they pose to patients. Therefore, the preferred method for detecting lactate biomolecules is through non-invasive means, which is considered the most reliable approach [3]. Scientists have conducted experiments on different bodily fluids, among which human sweat has emerged as a highly effective biomarker for non-invasive detection. This is because sweat provides a wide range of valuable information about an individual's health across various bodily fluids [4].

The energy metabolism of eccrine glands results in lactate production in sweat. As the intensity of exercise escalates, there is an increase in the production of lactate in sweat [5]. Therefore, sweat has the potential to accurately assess an individual's athletic capabilities without the need for intrusive blood sampling. Sweat lactate is a reliable indicator of tissue hypoxia and pressure ischemia due to its association with reduced oxidative metabolism and compromised tissue viability [6]. Lactate detection in perspired adult sweat presents new challenges due to the relatively small quantity and a broader range of physiologically significant lactate concentrations (4-30 mM).

Lab-based techniques such as gas chromatography (GC), liquid chromatography with mass spectrometric measurement (LC-MS), and high-pressure liquid chromatography (HPLC) can be employed for the detection of lactate [7]. Nevertheless, the cost of this equipment is frequently high, and the analytical procedures involved in sample treatment tend to be more protracted and arduous. In spectrophotometric measurements, the determination of lactate can be achieved through the utilization of the enzyme-mediated reactions of lactate oxidase and lactate dehydrogenase. However, it is important to acknowledge that certain drawbacks exist [8]. Therefore, the integration of electrochemical techniques with microfluidics has become increasingly prominent in contemporary research, primarily due to its advantages in rapid analysis, cost-

effectiveness, and minimal sample volume requirements [9].

The advancement of microfluidics technology has enabled the fabrication of compact devices that possess the ability to perform various functions such as particle and cell trapping, biomarker detection, nanomaterial production, droplet formation, and drug delivery [10]. Soft microfluidic devices have been developed for the purpose of sweat collection, sampling, and analysis. These types of tools are utilized for the instantaneous quantification of biomarkers. Therefore, there is a requirement for the advancement of cost-effective microfluidic sensors that possess efficient multiplexed electrochemical recognition capabilities [11].

This study employed an electrode, printed using an inkjet printing technique and modified with functionalized multi-walled carbon nanotubes. The purpose of this modification was to enable the non-invasive detection of lactate. A soft microfluidic channel composed of polydimethylsiloxane (PDMS) was constructed to facilitate the flow of the analyte being tested. The utilization of a three-electrode system was leveraged for electrochemical sensing. The working electrode (WE) was subjected to enzyme functionalization, while the reference electrode (RE) underwent modification using Ag/AgCl ink. Subsequently, electrochemical responses were recorded.

II. Experimental Section

A. Solutions and reagents

The lactate oxidase enzyme, Lactate, 1-Ethyl-3-(3-dimethyl aminopropyl) carbodiimide (EDC), N-hydroxy succinimide (NHS), MWCNT (Multi-walled carbon nanotubes), Potassium ferrocyanide, Potassium chloride was purchased from the Sigma Aldrich. PDMS (Polydimethylsiloxane) and curing agent were acquired from Dow Corning, USA. The Polyimide sheet was procured from Dali Electronics.

B. Development of the polyimide-based electrochemical sensor

For printing electrodes, a polyimide (PI) sheet was utilized. The stepwise fabrication methodology is given in Scheme 1. The dimensions of the three-electrode system were delineated and subsequently stored in the DXF file format. Subsequently, the DXF file underwent conversion into the Gerber file format utilizing the Dip Trace software. The converted file was uploaded into the Volterra software application for the purpose of printing. The calibration of the height and width of the nozzle was conducted. The utilization of optimized calibrated values was employed in the printing process of the device. The printed device was subjected to a temperature of 70°C for a duration of 15 minutes. The working and reference electrodes were subjected to modification using a multi-walled carbon nanotube and Ag/AgCl ink.

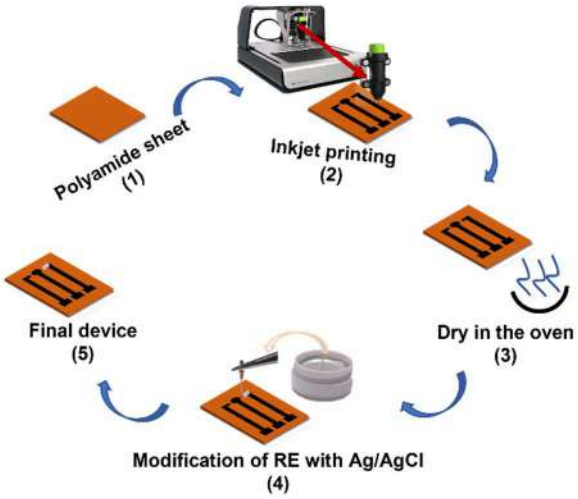

Scheme 1: Stepwise fabrication procedure for the fabrication of inkjet printed electrode

C . Development of enzyme-based lactate sensor

Initially, the working area of the electrode was subjected to a cleansing process by immersing it in PBS (Phosphate buffer solution) for a duration of 10 minutes, followed by air drying at ambient temperature [12]. Scheme 2 illustrates the schematic representation of the developmental process employed for the lactate sensor. A dispersion of functionalized multi-walled carbon nanotubes with a concentration of 2 mg/mL was prepared, which was subsequently modified by drop-casting 2 µl onto the working electrode. The modified dispersion was then allowed to dry at room temperature. Subsequently, the Lactate oxidase enzyme underwent crosslinking with the EDC/NHS crosslinker, specifically employing Carbodiimide cross-linkage on the modified electrodes. The sensor that was developed was stored at a temperature of 4°C for the duration of one night. The electrode was subsequently transferred to an electrolytic cell to facilitate electrochemical analysis.

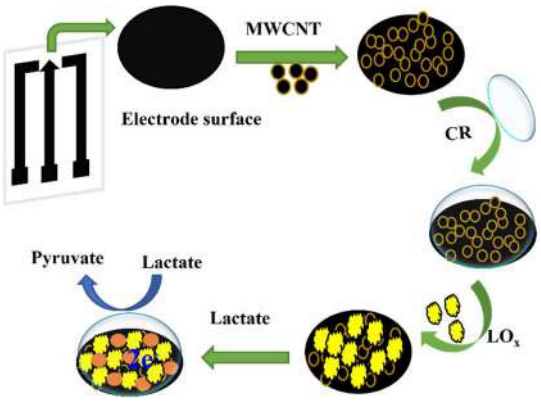

Scheme 2: Layer-by-layer modification of enzyme over the electrode surface. CR- Crosslinker reagent

D. Microfluidic channel development and its integration

A microfluidic channel was fabricated using soft lithography. The pattern of the requisite dimension was made in the CorelDraw software (Scheme 3). The PI sheet was affixed to the glass slide using adhesive tape and incised with a CO_2 laser to create a channel mold. The

polydimethylsiloxane was prepared by combining it with the curing agent in a ratio of 10:1. The mixture was dehydrated, subsequently poured onto the mold, and subjected to a temperature of 65°C for the purpose of solidification. The integration of PI-PDMS bonding was achieved through the utilization of irreversible bonding facilitated by an epoxy-thiol click reaction [14].

The microfluidic channel was treated for 10 min in the plasma and soaked in 1% MPTMS (3-mercaptopropyl trimethoxy silane) solution in methanol. Subsequently, the PDMS channel underwent a cleaning process using PBS solution followed by air-drying. A layer of epoxy adhesive was applied and aligned over the PI-based inkjet printer electrode, situated on the lowermost layer of the PDMS channel. To achieve the required irreversible bonding, three support plates are positioned on the PDMS channel's upper and lower surfaces for 12 hours.

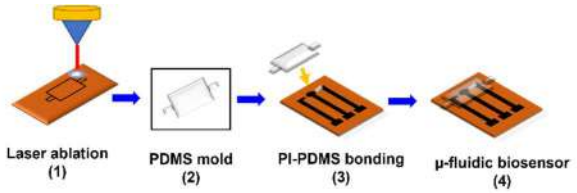

Scheme 3: Stepwise description for fabrication of microfluidic lactate sensor. (1) laser cut on the Polyimide substrate of required dimension adhered to the glass slide, (2) development of mold using PDMS and curing agent in the ratio of (10:1), (3) irreversible bonding of PDMS channel over the electrochemical sensor, (4) The integrated microfluidic device.

III. Results and Discussion

A. Sensor Characterization

The Scanning Electron Microscopy (SEM) technique was employed to investigate the surface morphology of both the bare carbon ink and the carbon ink modified with Multi-Walled Carbon Nanotubes. In the case of bare carbon ink, a planar morphology was observed (Figure 1a). However, upon modification with multi-walled carbon nanotubes, the morphology transformed into tube-like structures (Figure 1b). The modified structure exhibited a uniform distribution of homogenous tubes across the surface (Figure 1c and 1d). The elemental analysis was conducted to determine the carbon content and identify any additional impurities present. The carbon ink sample exhibited a carbon content of 88.76%, with the remaining 11.24% comprising various impurities such as nitrogen (N), oxygen (O), and chlorine (Cl). The carbon content was enhanced to 94.40% through the utilization of MWCNT modification.

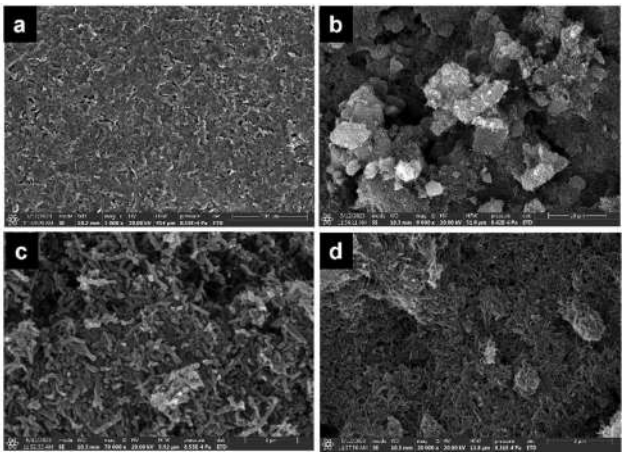

Figure 1: FESEM images of a) bare carbon ink and b, c, d) MWCNT modification over the carbon ink with different resolutions

B. Electrochemical characterization

The electrochemical characterization of the MWCNT-modified electrode was conducted utilizing an electrochemical experimental arrangement. To conduct a comparison between the reaction of unmodified and modified electrodes, cyclic voltammetry was carried out using a solution of potassium ferricyanide with a concentration of 5 mM in the presence of 0.1 M potassium chloride (KCl). At a scan rate of 0.05 V, the potential range extended from +1 to -1. The electrochemical response is depicted in Figure 2(a). The current response of the electrode was observed to increase twofold upon the modification of MWCNT in comparison to the unmodified electrode. This enhancement can be attributed to the improved surface coverage efficiency of the working electrode.

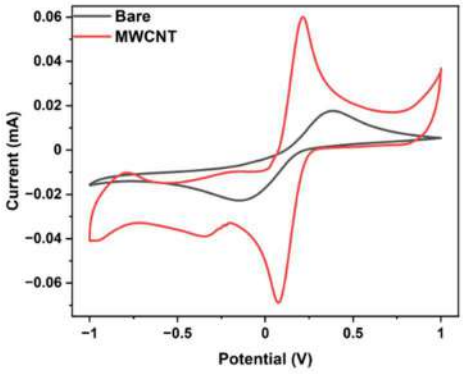

Figure 2. Cyclic Voltammetry of the bare electrode (black) and MWCNT-modified electrode (Red).

C. Biosensor performance

Cyclic voltammetry (CV) was performed after each modification step to ascertain the interfacial characteristics of the sensor that was developed. Figure 2(b) shows the CV response for each immobilized layer. The CV was performed in 5 mM $K_3Fe(CN)_6$ solution, with the addition of 0.1 M KCL, while carrying the voltage within the range of -0.6 to 0.8 V. The oxidation and reduction processes were detected at potentials of +0.23 V and -0.08 V, respectively. The electron transfer rate decreases,

decreasing the current values in CV because of modifying the layers.

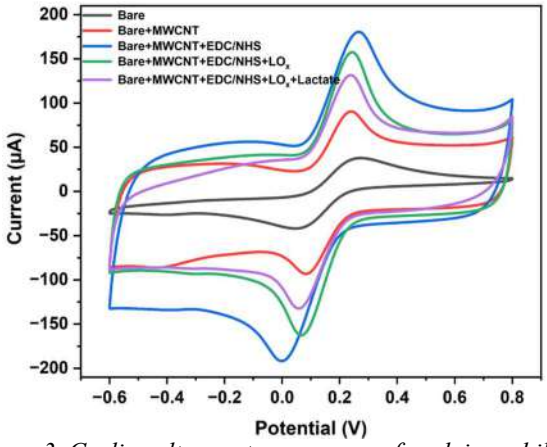

Figure 3. Cyclic voltammetry response of each immobilized layer bare electrode (Black), MWCNT modified (Red), EDC/NHS crosslinking (Blue), Lactate oxidase enzyme immobilization (Green), Lactate immobilization (Purple).

Figure 4 (a) represents the Differential Pulse Voltammetry (DPV) response of the sensor for a 1 mM – 20 mM lactate concentration. The observed potential (-0.375 V) at which the peaks were detected exhibited conformity with the results obtained from the cyclic voltammetry investigation. An elevation in the maximum value is observed when there is an increase in the concentration of lactate. In Figure 4 (b), the peak current and concentration are depicted for twenty different concentrations, demonstrating the linear behavior of the developed biosensor as the lactate concentration increases. The calibration plot of the Potential of anodic peak current vs. Concentration yielded a correlation coefficient value of $R^2 = 0.98$. The LoD and LoQ were determined using the given formulae:

$$\text{LoD/LoQ} = \frac{3.3/10 \times \sigma}{\text{Slope}}$$

The estimated LoD and LoQ of the developed devices are 1 and 3 mM, respectively.

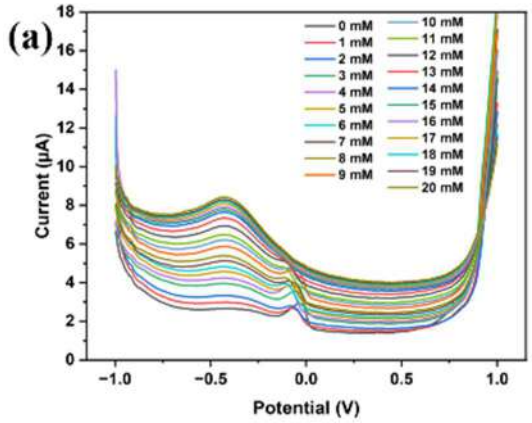

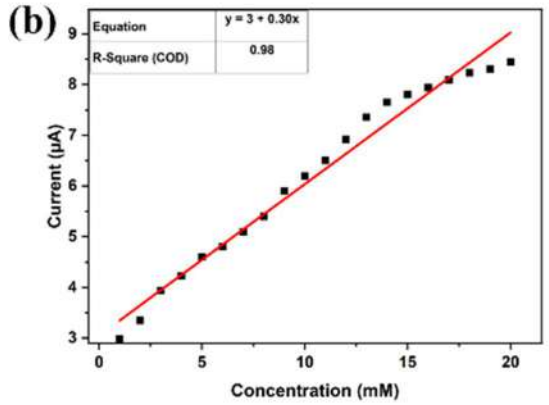

Figure 4 (a) DPV curve for lactate ranging from 1-20 mM. *(b) Calibration plot representing the direct relationship between concentration and peak current.*

C. Reproducibility study

The reproducibility of the lactate sensor was checked with four different devices. The study was carried out in a concentration of 5 mM. The electrochemical response was recorded for the four different devices, which showed reproducible peak potential, and the standard deviation was found to be 0.3% (≤10). Figure 5 shows the DPV results of the four different devices.

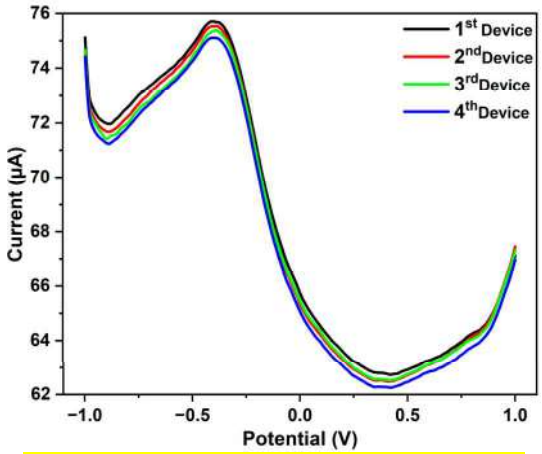

Figure 5. DPV curve for four different devices.

D. Interference study

The specificity of the developed sensor for the detection of lactate was checked using four different sweat analytes. The different analytes present in sweat, including glucose (8 mM), urea (50 mM), creatinine (2 mM), and uric acid (10 mM), were used. Figure 6 shows the current peak response of different analytes. As can be seen, the analytes in the sweat do not affect the sensor performance and selectivity of the developed lactate biosensor.

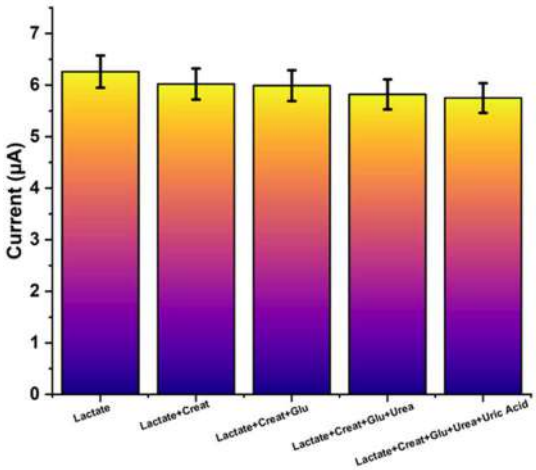

Fig 6 Histogram showing peak current response of the lactate and other interfering analytes.

E. Real-sample analysis

The artificial sweat sample was used for non-invasive detection of lactate. The artificial sweat sample was prepared according to ISO 3160-2 standards, and different concentrations of lactate (5, 10, 15, 20 mM) were spiked into the prepared sample. The electrochemical DPV response was checked for four spiked concentrations. The observed results are presented in Table 1. The average recovery was achieved in the 99-100 % range, and RSD values were between 0.06-0.25 %. These results show that the developed sensor has good accuracy in the detection of lactate.

Table 1. Detection of lactate in artificial sweat sample (n=3)

	Added (mM)	Found (mM)	Recovery (%)	RSD (%)
LACTATE	5	4.98	99.6	0.25
	10	10.01	100.1	0.17
	15	14.99	99.93	0.05
	20	19.97	99.85	0.06

IV. CONCLUSION

The current study focuses on the development of an inkjet-printed three-electrodes system for electrochemical sensing of lactate. In this system, the working electrode (WE) was subjected to modification using multi-walled carbon nanotubes (MWCNT), while the reference electrode (RE) was modified with silver/silver chloride (Ag/AgCl). MWCNTs offer a notable advantage in terms of their high surface area and effective capacity for material absorption. The integration of the microfluidic channel with a polyamide (PI)-based electrode was accomplished. The electrochemical analysis of the developed electrochemical sensor was conducted utilizing cyclic voltammetry (CV) and differential pulse voltammetry (DPV) techniques. The developed sensor demonstrates favorable sensing capabilities within the concentration range of 1-20 mM, exhibiting a Limit of Detection of 1 mM and a Limit of Quantification of 3 mM. The study has shown that the detected limit exhibits high specificity and sensitivity toward the electrode. In the future, improvement in sensor performance and its integration with wearable electronics will be carried out to detect various diseases and monitoring physical fitness.

ACKNOWLEDGMENT

The author immensely acknowledges the funding agency Indian Council of Medical Research for support (ICMR-SRF scheme 5/3/8/45/ITR-F/2022) and the BITS-Pilani Hyderabad campus central analytical laboratory for characterizations.

REFERENCES

[1] M. Braendlein *et al.*, "Lactate Detection in Tumor Cell Cultures Using Organic Transistor Circuits," *Advanced Materials*, vol. 29, no. 13, 2017, doi: 10.1002/adma.201605744.

[2] Q. Zhang *et al.*, "Wearable electrochemical biosensor based on molecularly imprinted Ag nanowires for noninvasive monitoring lactate in human sweat," *Sensors and Actuators, B: Chemical*, vol. 320, no. March, p. 128325, 2020, doi: 10.1016/j.snb.2020.128325.

[3] L. J. Currano, F. C. Sage, M. Hagedon, L. Hamilton, J. Patrone, and K. Gerasopoulos, "Wearable Sensor System for Detection of Lactate in Sweat," *Scientific Reports*, vol. 8, no. 1, pp. 1–11, 2018, doi: 10.1038/s41598-018-33565-x.

[4] X. Mei, J. Yang, X. Yu, Z. Peng, G. Zhang, and Y. Li, "Wearable molecularly imprinted electrochemical sensor with integrated nanofiber-based microfluidic chip for in situ monitoring of cortisol in sweat," *Sensors and Actuators B: Chemical*, vol. 381, no. December 2022, p. 133451, 2023, doi: 10.1016/j.snb.2023.133451.

[5] X. Xuan, C. Pérez-Ràfols, C. Chen, M. Cuartero, and G. A. Crespo, "Lactate Biosensing for Reliable On-Body Sweat Analysis," *ACS Sensors*, vol. 6, no. 7, pp. 2763–2771, 2021, doi: 10.1021/acssensors.1c01009.

[6] M. A. Djebbi, S. Boubakri, M. Braiek, N. Jaffrezic-Renault, P. Namour, and A. Ben Haj Amara, "High Performance Non-Enzymatic Electrochemical Lactate Sensor Based on ZnAl Layered Double Hydroxide Nanosheets Supported Gold

Nanoparticles," *Journal of The Electrochemical Society*, vol. 168, no. 5, p. 057529, 2021, doi: 10.1149/1945-7111/ac0226.

[7] R. Wang, Q. Zhai, T. An, S. Gong, and W. Cheng, "Stretchable gold fiber-based wearable textile electrochemical biosensor for lactate monitoring in sweat," *Talanta*, vol. 222, no. March 2020, p. 121484, 2021, doi: 10.1016/j.talanta.2020.121484.

[8] R. Vinoth, T. Nakagawa, J. Mathiyarasu, and A. M. V. Mohan, "Fully Printed Wearable Microfluidic Devices for High-Throughput Sweat Sampling and Multiplexed Electrochemical Analysis," *ACS Sensors*, vol. 6, no. 3, pp. 1174–1186, 2021, doi: 10.1021/acssensors.0c02446.

[9] M. Braendlein *et al.*, "Lactate Detection in Tumor Cell Cultures Using Organic Transistor Circuits," *Advanced Materials*, vol. 29, no. 13, 2017, doi: 10.1002/adma.201605744.

[10] X. Huang *et al.*, "Epidermal self-powered sweat sensors for glucose and lactate monitoring," *Bio-Design and Manufacturing*, vol. 5, no. 1, pp. 201–209, 2022, doi: 10.1007/s42242-021-00156-1.

[11] A. Martín *et al.*, "Epidermal Microfluidic Electrochemical Detection System: Enhanced Sweat Sampling and Metabolite Detection," *ACS Sensors*, vol. 2, no. 12, pp. 1860–1868, 2017, doi: 10.1021/acssensors.7b00729.

[12] W. Jia *et al.*, "Electrochemical tattoo biosensors for real-time noninvasive lactate monitoring in human perspiration," *Analytical Chemistry*, vol. 85, no. 14, pp. 6553–6560, 2013, doi: 10.1021/ac401573r.

[13] T. C. Pereira and N. R. Stradiotto, "Electrochemical sensing of lactate by using an electrode modified with molecularly imprinted polymers, reduced graphene oxide and gold nanoparticles," *Microchimica Acta*, vol. 186, no. 12, 2019, doi: 10.1007/s00604-019-3898-3.

[14] M. V. Hoang, H. J. Chung, and A. L. Elias, "Irreversible bonding of polyimide and polydimethylsiloxane (PDMS) based on a thiol-epoxy click reaction," *Journal of Micromechanics and Microengineering*, vol. 26, no. 10, 2016, doi: 10.1088/0960-1317/26/10/105019.

sensors

MDPI

Communication

Electromicrofluidic Device for Interference-Free Rapid Antibiotic Susceptibility Testing of *Escherichia coli* from Real Samples

Sonal Fande [1,2], Khairunnisa Amreen [1,3], D. Sriram [2], Valentin Mateev [4] and Sanket Goel [1,3,*]

[1] MEMS, Microfluidic and Nanoelectronics Lab, Department of Electrical and Electronics Engineering, Birla Institute of Technology and Science, Hyderabad 50078, India
[2] Department of Pharmacy, Birla Institute of Technology and Science, Hyderabad 500078, India
[3] Department of Electrical and Electronics Engineering, Birla Institute of Technology and Science, Hyderabad 500078, India
[4] Department of Electrical Apparatus, Technical University of Sofia, 1156 Sofia, Bulgaria
* Correspondence: sgoel@hyderabad.bits-pilani.ac.in

Abstract: Antimicrobial resistance (AMR) is a global health threat, progressively emerging as a significant public health issue. Therefore, an antibiotic susceptibility study is a powerful method for combating antimicrobial resistance. Antibiotic susceptibility study collectively helps in evaluating both genotypic and phenotypic resistance. However, current traditional antibiotic susceptibility study methods are time-consuming, laborious, and expensive. Hence, there is a pressing need to develop simple, rapid, miniature, and affordable devices to prevent antimicrobial resistance. Herein, a miniaturized, user-friendly device for the electrochemical antibiotic susceptibility study of *Escherichia coli* (*E. coli*) has been developed. In contrast to the traditional methods, the designed device has the rapid sensing ability to screen different antibiotics simultaneously, reducing the overall time of diagnosis. Screen-printed electrodes with integrated miniaturized reservoirs with a thermostat were developed. The designed device proffers simultaneous incubator-free culturing and detects antibiotic susceptibility within 6 h, seven times faster than the conventional method. Four antibiotics, namely amoxicillin–clavulanic acid, ciprofloxacin, ofloxacin, and cefpodoxime, were tested against *E. coli*. Tap water and synthetic urine samples were also tested for antibiotic susceptibility. The results show that the device could be used for antibiotic resistance susceptibility testing against *E. coli* with four antibiotics within six hours. The developed rapid, low-cost, user-friendly device will aid in antibiotic screening applications, enable the patient to receive the appropriate treatment, and help to lower the risk of anti-microbial resistance.

Keywords: antibiotic susceptibility testing; microfluidic; antimicrobial resistance; *E. coli*; multidrug resistance; minimum inhibitory concentration

Citation: Fande, S.; Amreen, K.; Sriram, D.; Mateev, V.; Goel, S. Electromicrofluidic Device for Interference-Free Rapid Antibiotic Susceptibility Testing of *Escherichia coli* from Real Samples. *Sensors* **2023**, *23*, 9314. https://doi.org/10.3390/s23239314

Academic Editor: Hugo Aguas

Received: 9 October 2023
Revised: 26 October 2023
Accepted: 10 November 2023
Published: 21 November 2023

1. Introduction

The accurate and early detection of microbial infection, followed by appropriate treatment via antibiotic administration, is pivotal in reducing the fatality and severity of the disease in a patient [1,2]. Antibiotics are effective against bacterial infection, by killing the bacteria or inhibiting its growth [3]. Alexander Fleming, a physics scientist, accidentally discovered the first antibiotic, penicillin, to treat bacterial infection. That simple discovery saved millions of lives over decades [4]. Since then, several antibiotics have been prepared and discovered over the years. However, with time, these microorganisms become resistant to drugs. Antimicrobial resistance arises when microbes do not have a more extended response to the medicine, making the infection harder to treat [5]. Therefore, with minimalistic symptoms and disease onset, it is crucial to identify the microorganism and

the antibiotic effective against it. An antimicrobial resistance (AMR) test is often conducted; AMR shows the type and quantity of antibiotic working against the microorganism [6].

Various pathogens, like bacteria, fungi, viruses, and parasites, cause infection and form resistance [7]. Among these, bacterial and viral infections are more prevalent [8]. Pneumonia, diarrhea, and urinary tract infections are the most pervasive bacterial illnesses caused by *Escherichia coli* [9]. *E. coli* is the most known bacterium that causes multidrug resistance [10]. Improper use of antibiotics, multiple illnesses, and prolonged stays in the hospital are critical risk factors for *E. coli* multidrug resistance [11]. Therefore, knowing the antibiotic effect, dosage, and duration before use is essential. Antibiotic susceptibility testing (AST) helps identify the pathogen and the most effective antibiotic against it [12,13]. AST provides information on selecting antibiotics and evaluates the minimum inhibitory concentration. It detects both phenotype and genotype resistance. Genotype is classified based on the presence or absence of a resistant gene, and phenotype is found without the gene mutation. Different techniques are available; among them, disk diffusion is the gold standard for AST, as is quick to execute, can identify many antibiotics in a single test, and allows for a wide range of antibiotic choices. Still, it takes time and cannot provide minimum inhibitory concentration values. Another method is broth dilution [14], which is straightforward, legitimate, and easily accessible but demands more supplies of reagents and introduces more room for error. Moreover, these traditional AST approaches are time-consuming and labor-intensive, requiring skilled laboratory set-up and bulky instrumentation [15]. Often, a time frame of 4–5 days is reportedly needed to study the resistance clinically. Owing to this, the infection increases, and sometimes delays can even be fatal [16]. Hence, developing rapid techniques for measuring antibiotic effectiveness will improve global health and decrease mortality [17]. In this context, miniaturized and microfluidics-based devices provide possible solutions [18,19]. Microfluidic-based devices offer multiple advantages of reduced assay time, low cost, simple operation, and increased testing efficacy [20,21]. However, some microfluidic devices need high resolution. A microfluidic device has recently been designed to separate microbial cells using a ferrohydrodynamic approach. However, the developed device is complex and requires more attention to the environmental effect on fluid flow inside the channel [22]. Hence, microfluidic integrated with electrochemical sensing further improves the detection efficacy and increases the simplicity and sensitivity of detection [23,24].

The present study is an extension of our previous work [25]. Herein, we developed a rapid, sensitive, miniaturized electrochemical device for simultaneous culturing, detection, and antibiotic susceptibility study [26,27]. Here, *E. coli* was used as a model microbe for testing the device. A screen-printed electrode system modified with graphitized mesoporous carbon (GMC) was used for testing [28]. GMC is a high surface area carbon material that helps sensitively detect *E. coli* [29,30]. The microfluidic channel was designed and integrated with screen-printed electrodes. The in-house laser-induced graphene (LIG) heater was fabricated to incubate bacterial culture. Various antibiotics were screened by checking the minimum inhibitory zone, and the one with a more significant inhibition zone was selected for susceptibility testing. Different antibiotic concentrations were prepared, and efficacy was checked using the electrochemical cyclic voltammetry (CV) method. The specificity of antibiotics towards *E. coli* was validated using *Streptococcus pneumoniae*, *Pseudomonas aeruginosa*, and *Shewanella putrefaciens* bacteria. The real sample analysis was done using artificial urine and water samples. The obtained results were further validated with the conventional broth dilution method. To the extent feasible, this is a benchmarking prototype study that has yet to be explored further. The strategy with further optimizations can also be used for other microorganisms in real-time. Figure 1 shows the mechanism of action of different antibiotics to prevent bacterial growth.

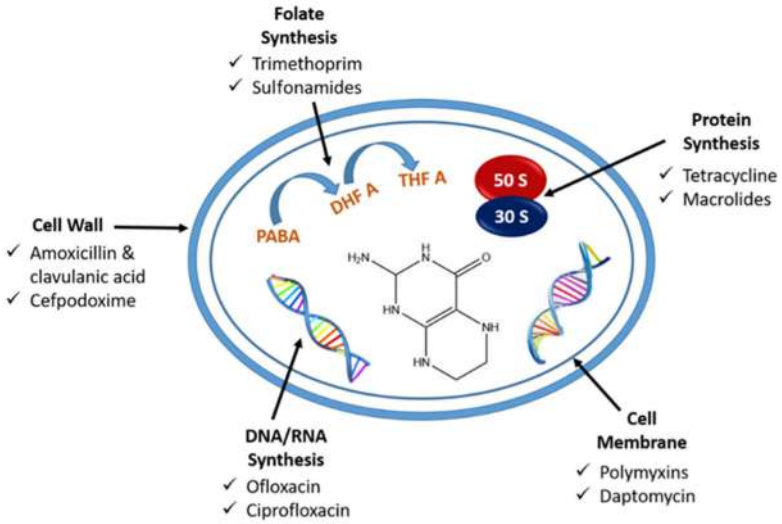

Figure 1. Schematic representation of the mechanism of action of antibacterial drugs.

2. Experimental Method

2.1. Materials

Luria broth and Luria agar were procured from Thermo Fisher Scientific, Delphi, India. Potassium chloride, carbon ink, glass slides (75 × 50 mm), ammonium phosphate, sodium sulfate, ammonium diphosphate, magnesium chloride, calcium chloride, creatinine, and urea were purchased from Sigma Aldrich, Ltd. (Burlington, MA, USA). *E. coli* culture was acquired from the Biological Science Department, BITS Pilani Hyderabad campus. Clavam 625 (amoxicillin and clavulanic acid), Zenflox 200 (ofloxacin), Monocef-O 200 (cefpodoxime), Cifran 500 (ciprofloxacin), and Azee-500 (azithromycin) were purchased from a local medical store. Polydimethylsiloxane (PDMS) was purchased from Delta Silicon, Mumbai, India. A CO_2 laser (VLS 3.20) was procured from Universal Laser Systems, Scottsdale, AZ, USA.

2.2. Development of Three-Electrode System and Microfluidic Device

A three-electrode system was fabricated using the screen-printing technique. The design of the requisite dimension was first drawn on SolidWorks software. A polyvinyl chloride (PVC) sheet was attached to a glass side (75 × 50 mm), and the laser was scribed over the PVC sheet to prepare the mask. Carbon ink was laid down over the obtained mask with the help of a squeeze and kept in the oven for 30 min at 60 °C. The PVC sheet was removed after drying, and the screen-printed electrodes were obtained [31]. Figure 2 depicts a detailed schematic of the fabrication process.

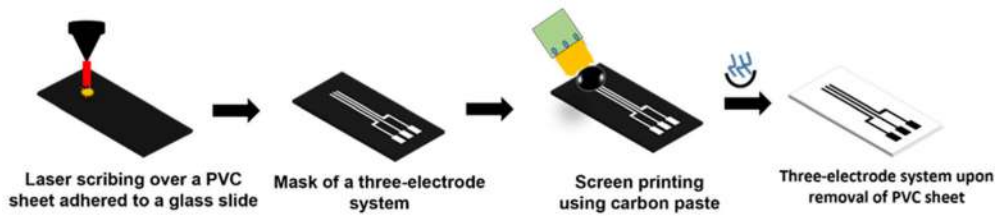

Figure 2. Schematic for the development of a three-electrode system using the screen-printing technique.

A mold (2 × 1.4 × 17 mm^3) was prepared on an acrylic sheet to develop the microfluidic device. To create a PDMS mixture, epoxy and curing agent were mixed in a 10:1 ratio and degassed for 30 min to remove oxygen bubbles. Following this, PDMS was run over the mold and baked for an hour at 60 °C. Post-curing, the reservoir was cut from the mold and bonded over the three-electrode system using the plasma bonding method. The developed

microfluidic device integrated with the laser-induced graphene (LIG) heater is shown in Figure 3. The details of the fabrication scheme for screen-printed electrodes, microfluidic device fabrication, and its integration, as well as how to prepare bacteria samples, were covered in greater depth in our previous research [25].

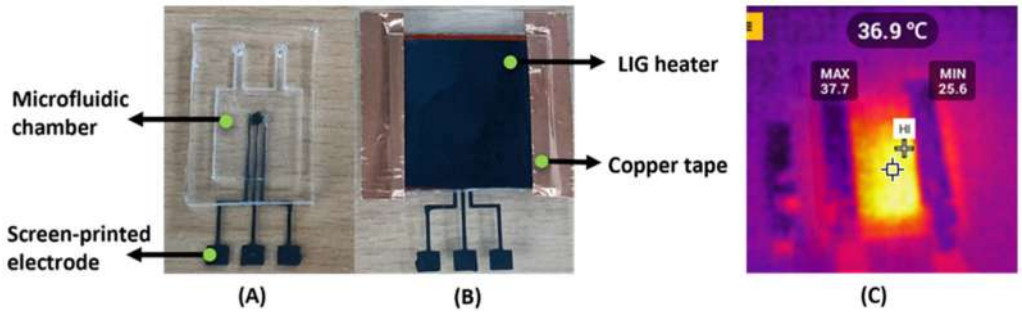

Figure 3. (**A**) A miniaturized device integrated with (**B**) a laser-induced graphene (LIG) heater provides temperature, and copper tape provides electrical contacts connected to the voltage regulator. (**C**) The LIG heater captured by a thermal camera after heating while providing a voltage of 2.5 V.

2.3. Fabrication of LIG Heater

For the fabrication of the LIG heater, a polyamide sheet of the required dimension of 25 × 25 mm was initially pasted onto a glass slide surface using double-sided tape. The CO_2 laser (VLS 3.60) was exposed on the polyimide sheet with power and speed of 6.5% and 4.5% to obtain laser-induced graphene [32]. After engraving, the obtained thickness was 50 µm. Electrical contacts were provided on the fabricated LIG film using copper tape and silver ink. The thermal factor was calibrated earlier by varying the potential and noting the temperature. A temperature of 37 °C was maintained by applying a potential of 2.5 V. A thermal camera was used to keep track of the achieved temperature. Figure 3C shows the temperature of the LIG heater, which was maintained at 37 ± 10 °C.

2.4. Effect of Antibiotic on E. coli

Electrochemical analysis was used to determine the effect of antibiotics on bacterial growth. A Potentiostat (CHI 1030E) was utilized to record the electrochemical response. A three-electrode setup was employed, with a reference electrode of Ag/AgCl, a working electrode of GMC, and a counter electrode of plan carbon ink.

2.5. Evaluation of Real Samples

The real samples used for analysis were synthetic urine and tap water [14]. The synthetic urine was prepared by adding all dried components to sterile water. Normal urine is a mixture of organic compounds such as urea, creatinine, and uric acid and inorganic substances like ammonia, sulfates, chloride, and phosphates. The composition of prepared synthetic urine is provided in Table 1.

Table 1. Composition of synthetic urine.

Components	Quantity (mg/L)
Potassium Chloride (KCl)	2000
Sodium Sulfate (Na_2SO_4)	2000
Ammonium Phosphate ($(NH_4)_3PO_4$)	850
Ammonium Diphosphate ($(NH_4)_3PO_4$)	850
Calcium Chloride ($CaCl_2$)	250
Magnesium Chloride ($MgCl_2$)	500
Urea (CH_4N_2O)	600
Creatinine ($C_4H_7N_3O$)	50

3. Results and Discussion

3.1. Off-Chip Minimum Inhibitory Concentration (MIC) Measurement

The MIC describes the resistance or susceptibility of the particular bacteria toward valuable antibiotics. The model microorganism used was *E. coli* (DH5α strain) for MIC calculation. An agar plate containing Luria–Bertani (LB) broth was used to sustain *E. coli* cells. A colony of *E. coli* cells was removed from the agar plate and suspended in 5 mL of LB liquid media. Overnight at 37 °C, the cells were cultured in the medium on a shaker at 200 rpm. After that, fresh LB medium was used to dilute the cell suspension until it reached an optical density of 0.01 at 600 nm.

The antibiotic stock solution (1 mg/mL) of cefpodoxime, ofloxacin, amoxicillin, clavulanic acid, and ciprofloxacin was prepared in sterile water. Several concentrations, ranging from 100 to 500 g/mL, were prepared from the stock solution, and the MIC was measured using a disk diffusion approach. The LB agar media was prepared and poured into a Petri plate. After solidifying the agar gel, the bacterial culture was spread over the plate. Using sterile forceps, an antibiotic disk of cefpodoxime, ofloxacin, amoxicillin, clavulanic acid, and ciprofloxacin was applied to the plate and incubated for 12 to 24 h at 37 °C. The minimum inhibition zone formed at the edge of the antibiotic disk was calculated. Figure 4 shows the disk diffusion method for MIC calculation. The distance from the antibiotic disk to the inhibition area for every antibiotic was calculated. The one that covered more inhibition zones, i.e., ciprofloxacin, was selected for a real sample and interference study.

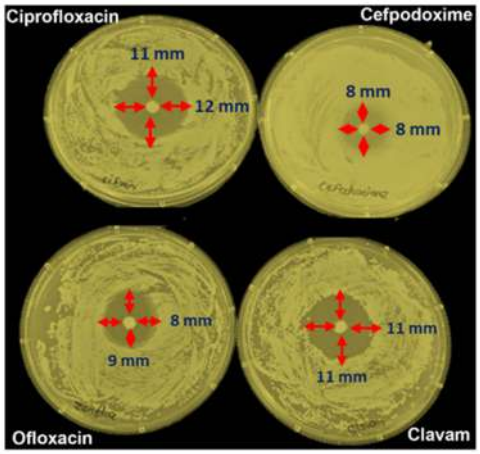

Figure 4. Disk diffusion method for calculation of minimum inhibitory concentration.

3.2. Electrochemical Detection of Antibiotic Effect over the Bacterial Growth

To carry out the electrochemical investigation of bacterial growth inhibition, 100 µg/mL antibiotic concentration of cefpodoxime, amoxicillin and clavulanic acid, ciprofloxacin, and ofloxacin with bacterial culture media was injected into four miniaturized reservoirs through the inlet. Before the analysis, the reservoir was washed with 0.1 M PBS to prevent cross-contamination. The LIG heater was used to incubate the bacterial culture throughout the experiment, which is necessary for bacterial growth. The electrochemical detection was carried out using CV for 6 h, and after every hour, the response was recorded. Figures 5 and 6 show the electrochemical reactions of the control sample (without antibiotic) and four antibiotics, and their respective calibration plots are given in Figure 7. According to the minimum inhibition zone study, out of four antibiotics, ciprofloxacin was more effective toward *E. coli* bacterial inhibition. The bacterial concentration would decline in the device with increased time and a constant temperature. In Figure 6, the current value increases with incubation time because of antibiotics on bacterial growth. Usually, when the bacteria grow, they accumulate over the electrode surface and block ion flow, decreasing the peak current value, which we can see in Figure 5 without antibiotic response. The antibiotic helps to increase the transfer of ions in the media, which was blocked by the growth of bacteria, as shown in Figure 6 [32].

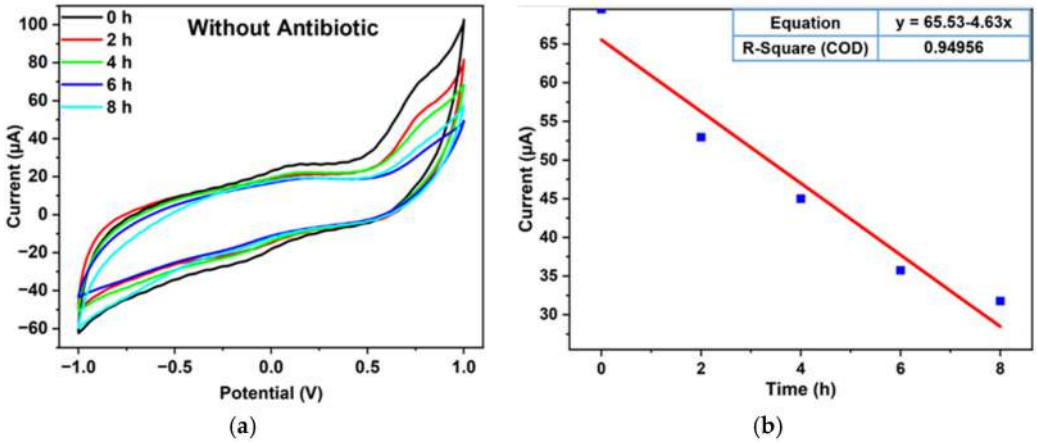

Figure 5. A cyclic voltammetric graph of bacterial culture without antibiotics (**a**) and its respective calibration plot (**b**).

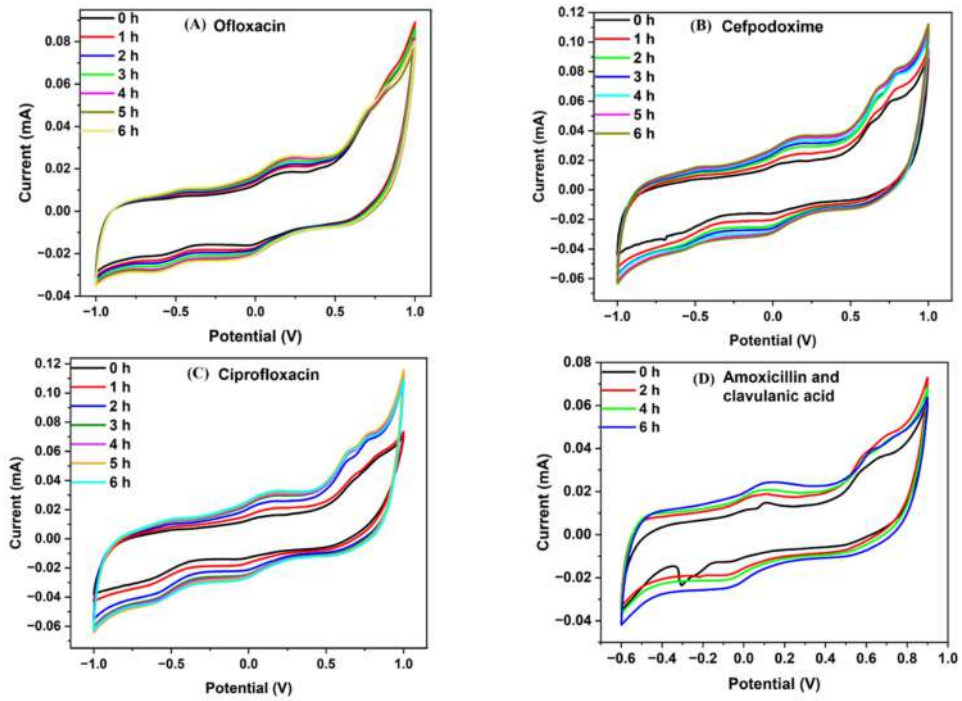

Figure 6. Cyclic voltammetric graphs of four antibiotics at concentrations of 100 µg/mL. The experiment was performed in the microfluidic device for 6 h, and the response was recorded at intervals every 1 h. (**A**) Ofloxacin, (**B**) cefpodoxime, (**C**) ciprofloxacin, (**D**) amoxicillin and clavulanic acid.

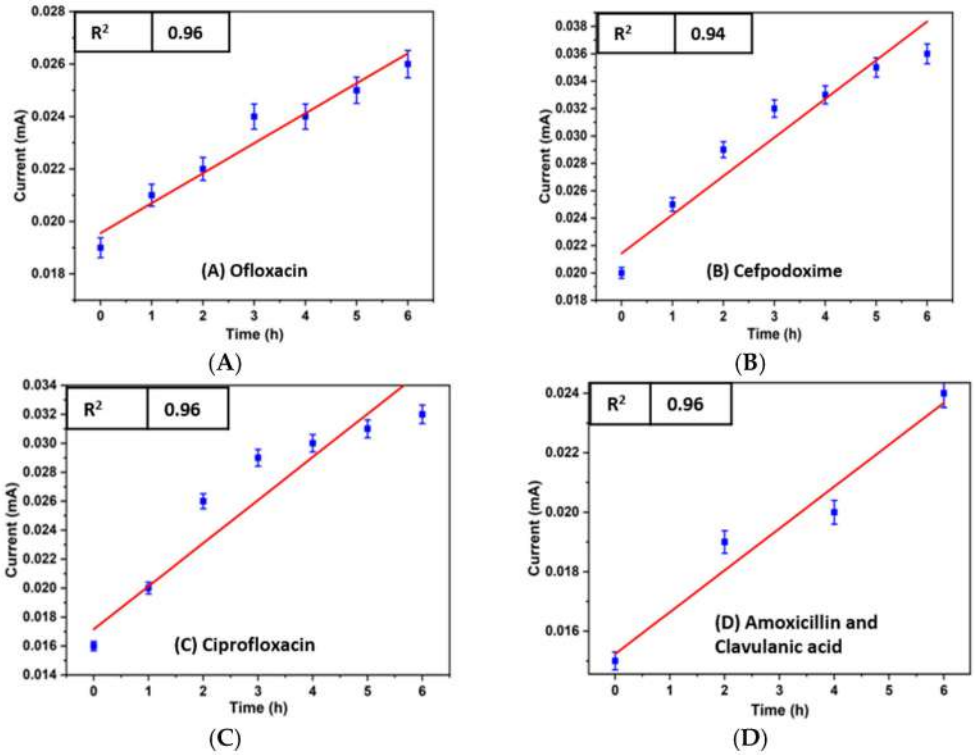

Figure 7. Calibration plot of four antibiotics was performed in the microfluidic device for 6 h. (**A**) Ofloxacin, (**B**) cefpodoxime, (**C**) ciprofloxacin, (**D**) amoxicillin and clavulanic acid.

3.3. Interference Study

The specificity of the Clavam antibiotic toward *E. coli* was checked in the developed microfluidic device. Four variants, namely *Streptococcus*, *Shewanella*, *Pseudomonas*, and *E. coli*, were tested with Clavam antibiotic. The first *E. coli* with Clavam antibiotic was injected into the device, and CV response was recorded, Figure 8a. *Pseudomonas*, *Streptococcus*, and *Shewanella* were then added into the same device, and the CV response was measured. A similar current histogram for *E. coli* and an additional variant mixed with *E. coli* is shown in Figure 8b. The apparent difference in the inhibition values for *E. coli* and other bacterial species confirms that ciprofloxacin did not affect *Shewanella putrefaciens*, *Pseudomonas aeruginosa*, and *Streptococcus pneumoniae* [25]. The efficiency of ciprofloxacin against different pathogens was negligible or less than 10%, indicating that it is solely effective against *E. coli* species or that the developed sensor is specific toward *E. coli* species.

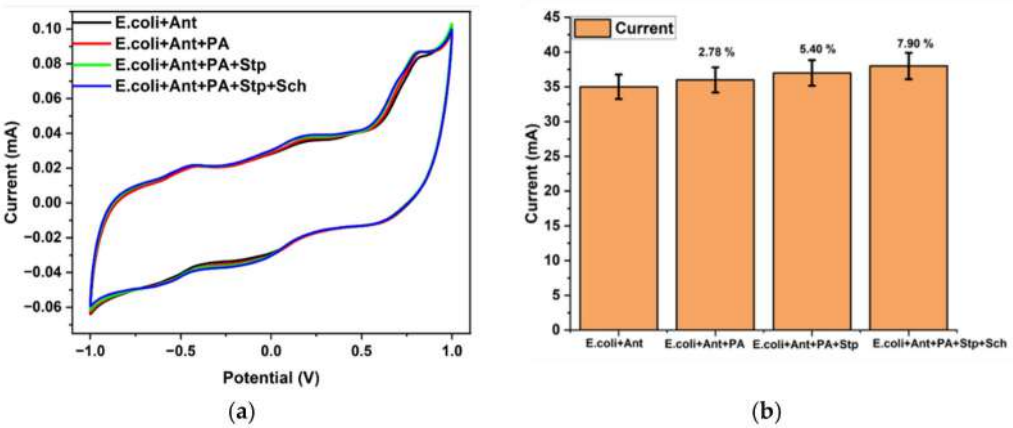

Figure 8. CV graph for specificity study of antibiotics (Ant) toward *E. coli*, *Pseudomonas aeruginosa* (PA), *Streptococcus pneumoniae* (Stp), and *Shewanella putrefaciens* (Sch). CV graph responses (**a**) and respective total current plot variation (**b**).

3.4. Antibiotic Susceptibility Testing Using Synthetic Urine

A urine sample is mainly used for examining a medical condition. However, obtaining the same quality urine for many illness detections takes time and effort. Hence, synthetic urine is used for experimentation purposes [33]. Along with this, water pollution due to microorganisms is also a significant issue that causes waterborne diseases. Therefore, there is a critical need to detect the microbial pollution of water [34]. Consequently, urine and water samples were selected for real sample analysis. Before testing, synthetic urine and tap water were autoclaved to avoid any microbial contamination.

E. coli culture was inoculated into the synthetic urine and tap water before being injected into the device. The electrochemical response was checked for 7 h at hourly intervals. The CV response of a water sample and synthetic urine is shown in Figure 9. The rise in current under the influence of antibiotics was observed [35]. As time increases, the current values also increase because the antibiotic decreases the growth of bacteria. The volume of ions in the urine increases the flow of ions, increasing the current value. This signifies the effect of antibiotics on the growth of bacteria.

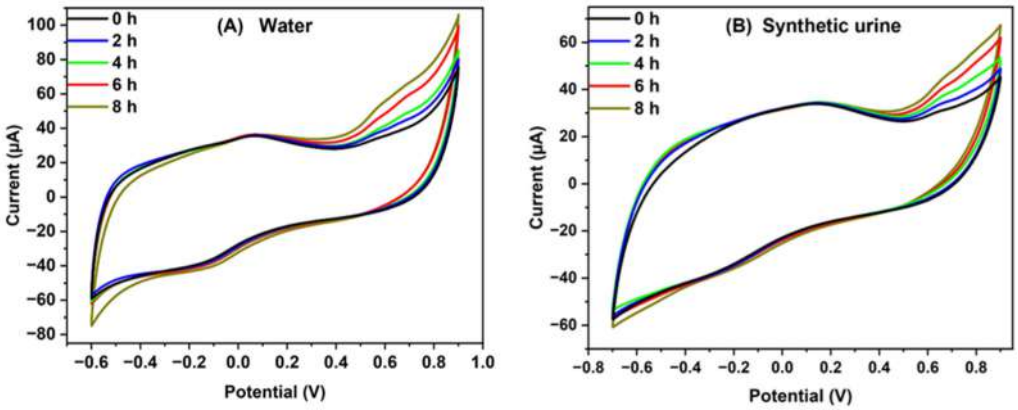

Figure 9. CV graph for real sample analysis performed in the microfluidic device for 7 h in (**A**) tap water and (**B**) synthetic urine.

4. Conclusions

This study developed a label-free, simple, cost-effective, miniaturized electrochemical microfluidic device to diagnose microbial resistance and bacterial infection rapidly. The designed device demonstrated remarkable sensitivity toward *E. coli* and detected the antibiotic susceptibility within a concise 6-h timeframe. As part of our methodology, a three-electrode system was added to our miniaturized platform, with the working electrode modified with GMC, the reference electrode using Ag/AgCl, and the counter electrode composed of bare carbon ink. Electrochemical detection was performed using cyclic voltammetry, which enabled accurate measurements. The working electrode was modified with GMC to improve sensor performance and increase precision. Four antibiotics of the same concentration were tested in the susceptibility study, and the interference of the antibiotic toward *E. coli* was detected. Further antibiotic susceptibility study was performed in both artificial urine and water samples, ensuring the versatility and robustness of our device's performance. The obtained outcomes were validated with the conventional approach, confirming the reliability of our findings. To address the pressing demand for rapid and accurate antibiotic susceptibility testing, integration with Cyber-Physical System (CPS) augmented techniques, like data mining and machine learning, with essential automation will aid in diagnosing antibiotic susceptibility rapidly. These technologies will advance the diagnostic process and enhance its accuracy. Moreover, as bacterial resistance to conventional treatments continues to rise, there is a critical need for technologies that accurately distinguish between resistant, susceptible, and persistent bacterial strains. These advancements pave the way for precision medicine, yielding optimal diagnostic results in the ever-evolving landscape of bacterial infections.

Author Contributions: Conceptualization, S.F., K.A., D.S., V.M. and S.G.; Methodology, S.F., K.A., D.S. and S.G.; Formal analysis, S.F., K.A., D.S., V.M. and S.G.; Investigation, S.F., K.A., D.S. and S.G.; Writing—original draft, S.F.; Writing—review & editing, K.A., D.S., V.M. and S.G.; Visualization, K.A., D.S. and S.G.; Supervision, K.A., D.S. and S.G. All authors have read and agreed to the published version of the manuscript.

Funding: This work was supported by the Indian Medical Council of Research Senior Research Fellow Scheme (ICMR-SRF scheme5/3/8/45/ITR-F/2022) and ICMR, Young Scientist Scheme, YSS/2020/000086.

Data Availability Statement: No new data were created or analyzed in this study. Data sharing is not applicable to this article.

Acknowledgments: The authors thank the funding agency (Indian Medical Council of Research) for financial support.

Conflicts of Interest: The authors declare no conflict of interest.

References

1. Yang, Y.T.; Wang, J.C.; Chuang, H.S. Developing Rapid Antimicrobial Susceptibility Testing for Motile/Non-Motile Bacteria Treated with Antibiotics Covering Five Bactericidal Mechanisms based on Bead-Based Optical Diffusometry. *Biosensors* **2020**, *10*, 181. [CrossRef]
2. Farshidfar, N.; Assar, S.; Amiri, M.A.; Sahmeddini, S.; Hamedani, S.; Zarei, M.; Tayebi, L. The Feasible Application of Microfluidic Tissue/Organ-on-a-Chip as an Impersonator of Oral Tissues and Organs: A Direction for Future Research. *Biodes. Manuf.* **2023**, *6*, 478–506. [CrossRef]
3. Verma, A.; Verma, M.; Singh, A. Animal tissue culture principles and applications. In *Animal Biotechnology*; Academic Press: Cambridge, MA, USA, 2020; ISBN 9780128117101.
4. Tarditto, L.V.; Zon, M.A.; Ovando, H.G.; Vettorazzi, N.R.; Arévalo, F.J.; Fernández, H. Electrochemical Magneto Immunosensor Based on Endogenous β-Galactosidase Enzyme to Determine Enterotoxicogenic *Escherichia coli* F4 (K88) in Swine Feces Using Square Wave Voltammetry. *Talanta* **2017**, *174*, 507–513. [CrossRef]
5. Pulingam, T.; Parumasivam, T.; Gazzali, A.M.; Sulaiman, A.M.; Chee, J.Y.; Lakshmanan, M.; Chin, C.F.; Sudesh, K. Antimicrobial Resistance: Prevalence, Economic Burden, Mechanisms of Resistance and Strategies to Overcome. *Eur. J. Pharm. Sci.* **2022**, *170*, 106103. [CrossRef]
6. Veloo, A.C.M.; Seme, K.; Raangs, E.; Rurenga, P.; Singadji, Z.; Wekema-Mulder, G.; Van Winkelhoff, A.J. Antibiotic Susceptibility Profiles of Oral Pathogens. *Int. J. Antimicrob. Agents* **2012**, *40*, 450–454. [CrossRef]
7. Karasinski, J.; White, L.; Zhang, Y.; Wang, E.; Andreescu, S.; Sadik, O.A.; Lavine, B.K.; Vora, M. Detection and Identification of Bacteria Using Antibiotic Susceptibility and a Multi-Array Electrochemical Sensor with Pattern Recognition. *Biosens. Bioelectron.* **2007**, *22*, 2643–2649. [CrossRef]
8. Pandey, A.; Gurbuz, Y.; Ozguz, V.; Niazi, J.H.; Qureshi, A. Graphene-Interfaced Electrical Biosensor for Label-Free and Sensitive Detection of Foodborne Pathogenic *E. Coli* O157:H7. *Biosens. Bioelectron.* **2017**, *91*, 225–231. [CrossRef]
9. Abu-Sini, M.K.; Maharmah, R.A.; Abulebdah, D.H.; Al-Sabi, M.N.S. Isolation and Identification of Coliform Bacteria and Multidrug-Resistant *Escherichia coli* from Water Intended for Drug Compounding in Community Pharmacies in Jordan. *Healthcare* **2023**, *11*, 299. [CrossRef]
10. Paulose, A.K.; Hou, Y.; Huang, Y.; Dileep, N.C.; Chiu, C.; Pal, A.; Kalaimani, V.M.; Lin, Z.; Chang, C.; Chen, C.; et al. Rapid Escherichia coli Cloned DNA Detection in Serum Using an Electrical Double Layer-Gated Field-Effect Transistor-Based DNA Sensor. *Anal. Chem.* **2023**, *95*, 6871–6878. [CrossRef]
11. Kumar, D.; Singh, A.K.; Ali, M.R.; Chander, Y. Antimicrobial Susceptibility Profile of Extended Spectrum β-Lactamase (ESBL) Producing *Escherichia coli* from Various Clinical Samples. *Infect. Dis. Res. Treat.* **2014**, *7*, IDRT.S13820. [CrossRef]
12. Behera, B.; Anil Vishnu, G.K.; Chatterjee, S.; Sitaramgupta, V.V.S.N.; Sreekumar, N.; Nagabhushan, A.; Rajendran, N.; Prathik, B.H.; Pandya, H.J. Emerging Technologies for Antibiotic Susceptibility Testing. *Biosens. Bioelectron.* **2019**, *142*, 111552. [CrossRef]
13. Cunha, A.P.; Henriques, R.; Cardoso, S.; Freitas, P.P.; Carvalho, C.M. Rapid and Multiplex Detection of Nosocomial Pathogens on a Phage-Based Magnetoresistive Lab-on-Chip Platform. *Biotechnol. Bioeng.* **2021**, *118*, 3164–3174. [CrossRef]
14. Jeon, H.; Khan, Z.A.; Barakat, E.; Park, S. Label-Free Electrochemical Microfluidic Chip for the Antimicrobial Susceptibility Testing. *Antibiotics* **2020**, *9*, 348. [CrossRef]
15. Webster, T.A.; Sismaet, H.J.; Chan, I.P.J.; Goluch, E.D. Electrochemically Monitoring the Antibiotic Susceptibility of *Pseudomonas aeruginosa* Biofilms. *Analyst* **2015**, *140*, 7195–7201. [CrossRef]
16. Ding, C.; Liu, Y.; Guo, Y.; Guo, X.; Kang, Q.; Yan, X.; He, Z. Precise Digital Bacteria Enumeration and Antibiotic Susceptibility Testing via a Portable Vibrating Capillary-Based Droplet Platform. *Sens. Actuators B Chem.* **2023**, *380*, 133254. [CrossRef]
17. Rao, R.P.; Sharma, S.; Mehrotra, T.; Das, R.; Kumar, R.; Singh, R.; Roy, I.; Basu, T. Rapid Electrochemical Monitoring of Bacterial Respiration for Gram-Positive and Gram-Negative Microbes: Potential Application in Antimicrobial Susceptibility Testing. *Anal. Chem.* **2020**, *92*, 4266–4274. [CrossRef]

18. Abbas, N.; Song, S.; Chang, M.S.; Chun, M.S. Point-of-Care Diagnostic Devices for Detection of *Escherichia coli* O157:H7 Using Microfluidic Systems: A Focused Review. *Biosensors* **2023**, *13*, 741. [CrossRef]
19. Kim, H.S.; Lee, H.; Park, J.; Abbas, N.; Kang, S.; Hyun, H.; Seong, H.; Yoon, J.G.; Noh, J.Y.; Kim, W.J.; et al. Collection and Detection of SARS-CoV-2 in Exhaled Breath Using Face Mask. *PLoS ONE* **2022**, *17*, e0270765. [CrossRef]
20. Mairhofer, J.; Roppert, K.; Ertl, P. Microfluidic Systems for Pathogen Sensing: A Review. *Sensors* **2009**, *9*, 4804–4823. [CrossRef]
21. Guo, J.; Wang, Y.; Xue, Z.; Xia, H.; Yang, N.; Zhang, R. Numerical Analysis of Capture and Isolation of Magnetic Nanoparticles in Microfluidic System. *Mod. Phys. Lett. B* **2018**, *32*, 1840075. [CrossRef]
22. Hewlin, R.; Edwards, M.; Smith, M. A 2D Transient Computational Multi-Physics Model for Analyzing Magnetic and Non-Magnetic Particle (Red Blood Cells and *E. Coli* Bacteria) Dynamics in a Travelling Wave Ferro-Magnetic Microfluidic Device for Potential Cell Separation and Sorting. *J. Eng. Sci. Med. Diagn. Ther.* **2023**, *7*, 021004. [CrossRef]
23. Besant, J.D.; Sargent, E.H.; Kelley, S.O. Rapid Electrochemical Phenotypic Profiling of Antibiotic-Resistant Bacteria. *Lab Chip* **2015**, *15*, 2799–2807. [CrossRef]
24. Grigorov, E.; Peykov, S.; Kirov, B. Novel Microfluidics Device for Rapid Antibiotics Susceptibility Screening. *Appl. Sci.* **2022**, *12*, 2198. [CrossRef]
25. Fande, S.; Amreen, K.; Sriram, D.; Goel, S. Microfluidic Electrochemical Device for Real-Time Culturing and Interference-Free Detection of *Escherichia coli*. *Anal. Chim. Acta* **2023**, *1237*, 340591. [CrossRef]
26. Tang, P.C.; Eriksson, O.; Sjögren, J.; Fatsis-Kavalopoulos, N.; Kreuger, J.; Andersson, D.I. A Microfluidic Chip for Studies of the Dynamics of Antibiotic Resistance Selection in Bacterial Biofilms. *Front. Cell. Infect. Microbiol.* **2022**, *12*, 896149. [CrossRef]
27. Zhang, Y.; Gholizadeh, H.; Young, P.; Traini, D.; Li, M.; Ong, H.X.; Cheng, S. Real-Time in-Situ Electrochemical Monitoring of *Pseudomonas aeruginosa* Biofilms Grown on Air–Liquid Interface and Its Antibiotic Susceptibility Using a Novel Dual-Chamber Microfluidic Device. *Biotechnol. Bioeng.* **2023**, *120*, 702–714. [CrossRef]
28. Chikezie, I.O. Determination of Minimum Inhibitory Concentration (MIC) and Minimum Bactericidal Concentration (MBC) Using a Novel Dilution Tube Method. *Afr. J. Microbiol. Res.* **2017**, *11*, 977–980. [CrossRef]
29. Altintas, Z.; Akgun, M.; Kokturk, G.; Uludag, Y. A Fully Automated Microfluidic-Based Electrochemical Sensor for Real-Time Bacteria Detection. *Biosens. Bioelectron.* **2018**, *100*, 541–548. [CrossRef]
30. Song, K.; Yu, Z.; Zu, X.; Huang, L.; Fu, D.; Yao, J.; Hu, Z.; Xue, Y. Microfluidic Chip for Detection of Drug Resistance at the Single-Cell Level. *Micromachines* **2023**, *14*, 46. [CrossRef]
31. Srikanth, S.; Jayapiriya, U.S.; Dubey, S.K.; Javed, A.; Goel, S. A Protocol to Execute a Lab-on-Chip Platform for Simultaneous Culture and Electrochemical Detection of Bacteria. *STAR Protoc.* **2023**, *4*, 102327. [CrossRef]
32. Srikanth, S.; Jayapiriya, U.S.; Dubey, S.K.; Javed, A.; Goel, S. Lab-On-Chip Integrated Platform with Screen Printed Electrodes and Laser Induced Graphene Heater for Simultaneous Culture and Electrochemical Detection of Bacteria. Available online: https://ssrn.com/abstract=4024173 (accessed on 1 September 2023).
33. Haddad, L. Synthetic Urine and Method of Making Same. US Patent 7,109,035 B2, 19 September 2006.
34. Some, S.; Mondal, R.; Mitra, D.; Jain, D.; Verma, D.; Das, S. Microbial Pollution of Water with Special Reference to Coliform Bacteria and Their Nexus with Environment. *Energy Nexus* **2021**, *1*, 100008. [CrossRef]
35. Luo, J.; Fang, X.; Ye, D.; Li, H.; Chen, H.; Zhang, S.; Kong, J. A Real-Time Microfluidic Multiplex Electrochemical Loop-Mediated Isothermal Amplification Chip for Differentiating Bacteria. *Biosens. Bioelectron.* **2014**, *60*, 84–91. [CrossRef]